Journal of Materials Research and Technology 33 (2024) 7681–7697

Contents lists available at ScienceDirect

Journal of Materials Research and Technology

journal homepage: www.elsevier.com/locate/jmrt

Mitigating hydrogen embrittlement in high-entropy alloys for next-generation hydrogen storage systems

V. Balaji [a], P. Jeyapandiarajan [a], J. Joel [a], Arivazhagan Anbalagan [b], P. Ashwath [b], S. Margret Anouncia [a], Andre Batako [c], M. Anthony Xavior [a,*]

[a] Vellore Institute of Technology, Vellore, Tamil Nadu, 632014, India
[b] Coventry University, United Kingdom
[c] Liverpool John Moores University, United Kingdom

ARTICLE INFO

Keywords:
High entropy alloys
Hydrogen storage
Hydrogen embrittlement (HE) mechanisms
Phase stability

ABSTRACT

Green hydrogen can potentially reduce carbon emissions in several types of automotive, transport and energy industries. However, effective handling of hydrogen during generation, storage, transportation, and distribution poses significant challenges concerning the materials aspect as they are prone to failure. One of the primary reasons for the failure of material is hydrogen embrittlement (HE). This review focuses on developing a new alloy system namely high-entropy alloys (HEAs) to improve and promote microstructure modifications and enhance mechanical properties. Researchers have developed many high-entropy alloys (HEAs) for handling hydrogen to overcome the failure faced by conventional materials. The primary cause of HE in materials is the absence of phase stability and crystal structure changes during hydrogen-induced environments. However, increasing the materials' ductility is more likely to reduce HE failures. Thus, FCC crystal structures are preferred for hydrogen storage materials. Adding multiple elements to increase the entropy level, which supports high-phase stability in all environmental conditions, is an important reason for using HEAs to mitigate HE failures.

1. Introduction

In 2004, Cantor and Yeh proposed the development of high-entropy alloys (HEAs), which was considered a significant advancement in materials science engineering for better strength-ductility trade-off. This innovative HEAs concept entails integrating significant quantities of various elements, usually ranging from 4 to 13 element addition in approximately equal or near equal proportions, to produce alloys with distinct properties. Yeh strongly recommends adding various elements to enhance the entropy level of the alloy system, for that results to reflect the mechanical property development [1,2]. Combining four or more elements in a single-phase solid solution, which can be either partially ordered or disordered, accomplishes this result. Furthermore, there is a reduced likelihood of intermetallic compound formation in HEAs. The development of alloy formation depends on Gibbs free energy. It considers factors such as enthalpy of mixing, temperature, and entropy of mixing [3]. By reducing their enthalpy, entropy plays a critical role in determining the lifespan or efficiency of systems. This type of entropy for developing alloy systems is converted into low, medium, and high entropy alloys, based on the above classification, depending on entropy generation and the addition of various elements [4]. HEAs have garnered significant interest in recent years due to their exceptional properties, such as high hardness, improved thermal stability, enhanced strength, and balance between strength-to-ductile ratios. This type of mechanical property development is based on four distinct types of HEAs-effects: high entropy effect, several lattice distortion effect, sluggish diffusion effect, and cocktail effect [5]. The high entropy effect is employed to generate entropy and the lattice distortion effect to account for variations in atomic size [6]. The sluggish diffusion effect is used to slow down the diffusion rate and employ the cocktail effect to create unexpected synergies [7]. The properties of HEAs are determined by considering additional factors, such as atomic size mismatch (δ), electronegativity, valence electron concentration (VEC), enthalpy (H), and enthalpy (S) production [8]. In hydrogen storage applications, the parameters VEC, δ, H, and S hold greater significance for property evaluation [9]. **Since** hydrogen has high energy density and many countries focus on green hydrogen development, the demand for effective hydrogen storage materials is increasing. Limitations include high

* Corresponding author.
E-mail address: manthonyxavior@vit.ac.in (M. Anthony Xavior).

https://doi.org/10.1016/j.jmrt.2024.11.139
Received 10 July 2024; Received in revised form 12 November 2024; Accepted 14 November 2024
Available online 17 November 2024

production costs, storage and transportation issues, poor volumetric density, etc. Production and transit in energy storage applications significantly impact energy density. The energy density of hydrogen ranges from 120 to 142 MJ kg^{-1}. The effects of high energy density include storage difficulties, safety problems, and infrastructure challenges [10]. Despite the restrictions, hydrogen is highly appealing to the globe because of its role in the renewable energy revolution, cost-effectiveness, environmental cleanliness, and decarbonisation potential [11]. Hydrogen storage applications must meet thermodynamic interaction requirements for hydrogen pressure, temperature, and electrode potential. Hydride-forming elements play a crucial role in enhancing and optimizing hydrogen storage systems. These types of elements' characteristics easily absorb and then readily release hydrogen, so the accumulation of hydrogen is not possible at grain boundaries. The hydrogen storage capacity varies depending on the alloying addition chosen. Each element combines with two hydrogen atoms to create a compound known as dihydride MH_2. The hydrogen storage capacity determines the performance evaluation. Overall, alloys with more than 2 atomic units exhibit greater efficiency in hydrogen storage and transport applications [12]. The first study in 2010 concentrated on the development of HEAs in hydrogen storage, followed by a study of TIVZrNbHf-based HEAs, with a capacity of 2.5 atomic units. The atomic units in the study represent the capacity of hydrogen storage [6], HEAs made up of elements with a higher atomic mismatch are more useful for hydrogen-based applications because of a higher atomic mismatch and higher diffusion of hydrogen [13]. Hydrogen enters materials, causing damage and failure to various engineering components and energy storage devices. The failure of the material is in the form of hydrogen embrittlement (HE), hydrogen-induced cracking (HIC), and high-temperature hydrogen attack (HTHA). When HE happens, it changes the mechanical properties of the alloy, lowering its toughness, ductility, and strength. It can also cause catastrophic failure, spread cracks on the surface, and make parts like pressure vessels, tubes, pipelines, and nuclear systems less reliable. High-strength alloys and materials frequently fail in hydrogen environments due to the propensity of hydrogen atoms to lower material strength. Also, the alloying system's crystal structure is one of the factors influencing susceptibility to HE. Compared to the FCC crystal structure, the BCC and HCP structures have a greater impact on the HE. It is noted that FCC exhibits good toughness, corrosion resistance, and a higher percentage of ductility, all of which significantly contribute to the hydrogen-enhanced decohesion process. BCC and HCP crystals have high hardness, strength, and hardness. Followed by reduced plasticity, high-strength materials easily affect embrittlement failures [14]. Low-alloy and carbon steels' BCC lattices have extremely high hydrogen mobility. The materials receive a source of hydrogen that develops a HE. Fig. 1 illustrates the two possible (internal and external) means by which hydrogen enters the materials (see Fig. 2).

At macro and microscopic levels, the limitations of hydrogen-absorbing materials affect their tensile strength, fracture toughness, and fatigue strength. Materials such as aluminium alloys, super alloys, low alloys, and precipitation hardening steels are mostly affecting this type of HE. This review discusses hydrogen-related phenomena, including hydrogen adsorption, diffusion, and characterization. Most hydrogen storage applications and transport sectors, such as maritime and road-borne haulage, use the term hydrogen embrittlement to rectify this issue with HEAs. This type of problem accounts for the majority of failures. Furthermore, there are possibilities for hydrogen storage using physical (liquid hydrogen, compressed gas, cryo, or cold compressed) and material (physisorption and chemisorption) methods [10].

2. Need for the design and development of hydrogen storage systems

2.1. Role of hydrogen in the future

In the future, renewable energy will lead the world. From 1970 to 2020, world power generation depended on hydropower, nuclear energy, oil, gas, and coal as major sources. However, between 2020 and 2050, fossil fuels, renewable energy sources, and solar and wind energy will all help meet the world's energy needs. The development of all new energy sources relies on reducing CO_2 emissions. Industrial activities generate approximately 30% of CO_2 emissions, according to research by the Intergovernmental Panel on Climate Change (IPCC). Commercial and residential (23%). Electricity production (21%). The transport sector accounts for (19%), while agriculture accounts for 6%. Following the National Automotive Policy 2020, the agenda is to minimize carbon emissions in road transport sectors, and the aim is for the ASEAN region's fuel economy to be 5.3 L (light gasoline equivalent) for 100 km by 2025.

2.2. Methods of hydrogen storage based on the physical form

Efficient hydrogen storage is a critical element in the hydrogen handling process for various applications. The storage of hydrogen utilizes both physical and material-based approaches. It included compressed gas, cryo-compressed gas, and liquid hydrogen stored in a physical-based method. Materials-based hydrogen storage mechanisms include physisorption and chemisorption. The consumer views the process of obtaining materials as a means of meeting shared requirements. The criteria include high efficiency, high life span, refusal time, and cost factors [15]. Two categories of hydrogen storage applications exist, namely stationary and mobile applications [16]. As the name suggests, stationary is an on-site or stationary power generation

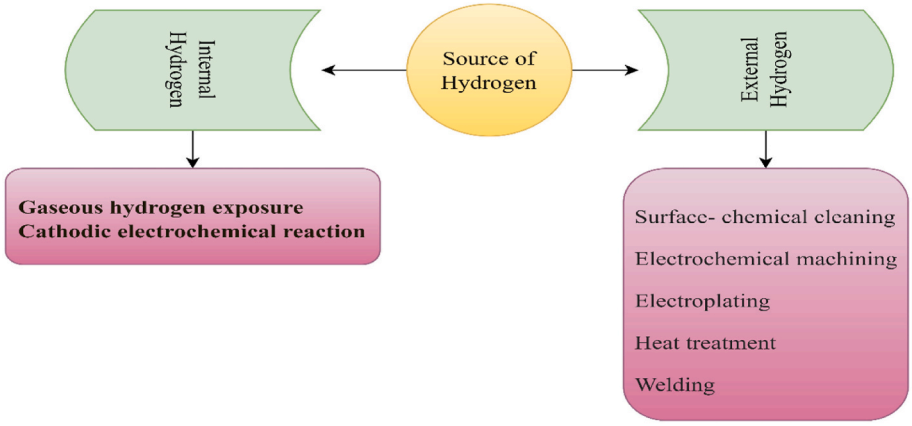

Fig. 1. Two Possible means by which Hydrogen enters the materials.

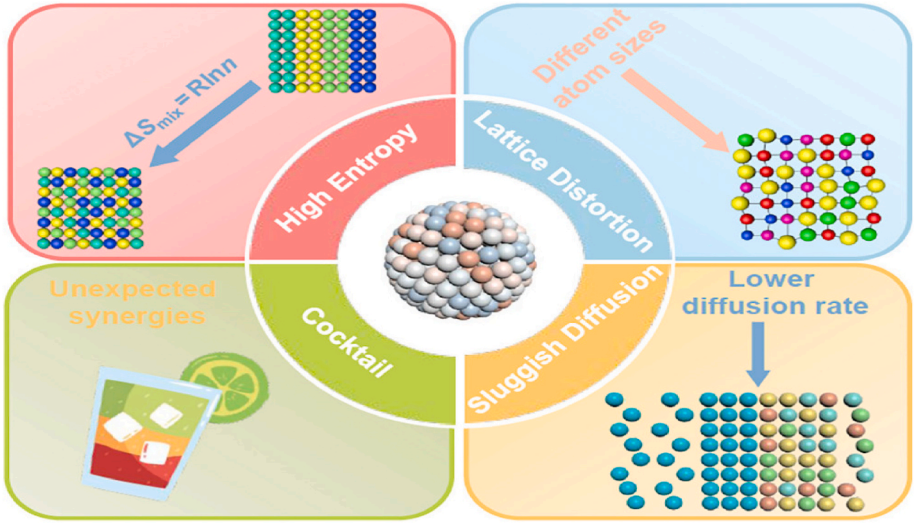

Fig. 2. Various core effects of HEAs [7]. Reuse with journal permission. Copyrights 2024, ACS publications.

application. Mobile transport of hydrogen from one location to another is possible with the help of a bulk-hydrogen storage tank or equipment due to the lower heating value of hydrogen (9.9 MJ/m^3). The future goal is to construct a high-quality hydrogen storage system that meets specific criteria to manage the tank's high pressure and low temperature.

2.2.1. *Liquid hydrogen*

Even at atmospheric pressure levels, liquid-type hydrogen has the advantage of getting stored at a high density. The hydrogen has a pressure of 0.1 MPa and a density of 70 kg/m3 [17]. During internal compression, the hydrogen density is increased. The temperature of hydrogen is near −250 °C. Hydrogen in a liquid state is becoming more and more difficult for effective storage systems to maintain. Furthermore, effective storage conditions for ammonia and liquid organic hydrogen carriers (LOHCs) are less rigorous [18].

2.2.2. *Compressed gas*

This method of storage is very efficient compared to other physical-based storage methods due to its high energy efficiency [19,20]. Four types of hydrogen storage vessels have been used recently. These vessels are referred to as type 1 pressure vessel, type 2 pressure vessel, type 3 pressure vessel, and type 4 pressure vessel. Pure metal makes up the type 1 vessels. Compared to other types, they are most common and less expensive to manufacture. Usually made of aluminium and steel materials. They can withstand pressure levels up to 50 MPa. Steel forms the outside surface of Type 2 vessels, which cover the glass fiber composite. Compared to type 1 vessels, they are 50 % more expensive to manufacture and 40% lighter. Type 3 is entirely made of carbon fiber composite wrapped in metal which can withstand a pressure up to 45 MPa, and failure starts at over 70 MPa. Compared to Type 2, they are twice as expensive to handle. Type 4 consists entirely of composite materials, with the liner composed of non-metals such as polymers or high-density polyethylene. It is constructed from materials that are both lightweight and costly which can withstand pressure levels as high as 100 MPa [16].

3. Different hydrogen charging techniques

Hydrogen is induced into the alloy system using two methods (i) electrochemical (liquid hydrogen) and (ii) gas hydrogen charging. One of the main reasons for HE failures occurring inside the materials are diffusion of hydrogen inside the materials. The diffusion of hydrogen strongly changes the material's behaviour in brittle form. This HE failure behaviour changes from various hydrogen-diffusion conditions.

3.1. *Electrochemical hydrogen charging*

The electrochemical hydrogen charging method is also called cathodic hydrogen charging. For electrochemical charging, samples are immersed inside the electrolytic solution. This type of electrolytic solution initiates the hydrogen reactions inside the samples. Various factors influence the reaction of the sample surface to the core. They are temperature, charging current, charging duration on the sample, and electrolytic concentrations. For this type of charging various electrolytic solutions are prepared based on the requirements [21]. This includes 1 equivalent of H_2SO_4 (sulfuric acid), HCL (hydrochloric acid), and NaOH (Sodium hydroxide) mixed with 1 L of solution and various concentrations with constant current density for various charging durations [22]. This type of charging contains various types of electrodes like working electrode, counter electrode, and reference electrode. The purpose of using the electrode is to improve the reaction and increase the efficiency of the electrolytic and sample efficiency. Platinum-type electrodes are highly reactive and mostly used in electrochemical hydrogen charging, gold, zinc, nickel, and lead types of electrodes are mostly used for high conductivity, corrosion protection, and batter-based applications.

3.2. *Gas hydrogen charging*

In gaseous hydrogen charging, at the time of hydrogen transportation through pipelines made of high-strength alloy materials, the mechanical property is decreased due to crystal structure changes by the influence of hydrogen absorption in the pipeline materials and develops a hydrogen embrittlement failure. The development of hydrogen embrittlement failure in the pipeline or other transportation or storage equipment depends on the purity of hydrogen gas, pressure, and temperature levels, alloy compositions, gaseous hydrogen charging time, trapping of hydrogen, and various stress concentration levels. In gaseous hydrogen charging, samples are located inside the pressure vessels. The pressure vessels are filled with hydrogen gas under different pressure and temperature conditions. During the gaseous hydrogen exposure, the addition of a minor amount of SO_2, O_2, and CO gaseous is one of the possible reasons for the reduction of HE in the pipeline because the addition of these gaseous elements acts as good inhibitors for HE [23]. The possible results of gaseous phase hydrogen charging have slightly increased the interstitial strengthening behaviour of the materials. Interstitial strengthening and work-hardening rate (WHR) are highly related to improving mechanical property development. The materials subjected to high WHR enhance the high yield and wear, improve the % of ductility, and delay crack initiation [24]. The WHR and YS increases

are advantages for the reduction of HE based on the factors (i) development of nano-twins according to low SFE in hydrogen-induced conditions, (ii) movement of drag force near the dislocation movement. Compared to electrochemical hydrogen charging the gaseous hydrogen charging methods increase the mechanical properties such as yield strength and also reduce the HE failures [25].

4. Recent trends in high-entropy alloys: Unveiling the potential of multi-element materials

4.1. High entropy alloys

Energy saving should be the primary criteria to be considered while developing new materials for different applications and in this direction, a new alloy system called HEAs [26] are introduced. The addition of individual principal elements is between 5 and 35 at% in equiatomic or non-equiatomic proportion. The combined nature of strength and ductility is a unique property for selecting HEAs in structural and hydrogen storage applications. Moreover, HEAs and their components are used in catalysis, high temperature, corrosion resistance, high thermal stability, magnetic materials, etc [27].

4.2. Overview of phase formation criteria of HEAs

Entropy-based alloy systems vary from principal element addition like $\triangle S \leq 1.0R$ for low entropy alloys, $1.0R \leq \triangle S \leq 1.5R$ for medium entropy alloys, and $\triangle S \geq 1.5R$ for high entropy alloys [3]. Based on the above-mentioned entropy ranges of the alloys, their hydrogen storage capacity and resistance to hydrogen embrittlement behavior are different. The development of HEAs is based on various factors, such as alloy formation rules, various core effects of HEAs, and fabrication methods. Gibbs free energy is a basic alloy formation rule for developing HEAs.

$$\Delta G_{mix} = \Delta H_{mix} - T\Delta S_{mix} \quad (1)$$

Reduction in mixing enthalpy (ΔH_{mix}) of the system to enhance the mixing entropy (ΔS_{mix}) of the alloys. Different phases are formed in conventional alloy systems, including terminal solutions, intermediate solutions, and intermetallic compounds. The terminal solutions completely disperse the element addition in the base metals, preventing the development of separate phases. After fabricating base metals under varying pressure-temperature conditions, intermediate solutions need to specify the range of composition between individual element additions and distinct microstructures in the various phases. For intermetallic compounds, the addition of different metals or metalloids is necessary to achieve an ordered structure with high strength and hardness [28]. For the HEAs system, various phases are formed, such as simple or random solid solutions, e.g., FCC and BCC structures. Super lattices/Ordered solid solution, e.g., B_2 and $L1_2$, C12 – W, cF4-Cu, hP2-Mg, and Intermetallic phases, e.g., laves phases, σ, and μ structure, are formed [28,29]. Moreover, the HEAs are further converted into (i) Simple disordered phase (SDP), (ii) Simple ordered phase (SOP), and (iii) Complex ordered phase (COP). Table 1 represents the various parameters and their acceptable values for the formation of a simple disordered phase (SDP).

These types of phases are formed in HEAs depending on the enthalpy of mixing (Hmix), the entropy of mixing (Smix), and atomic size differences (δ). Table 2 represents the various parameters, and their considerable values forming simple and complex ordered phases (SOP and COP).

Valence electron concentration (VEC), Pauling electronegativity difference (Δ_X), and mobile electron concentration (e/a) are empirical criteria for the prediction of phase structure in HEAs. VEC <6.8 for BCC structure, VEC >8 for FCC, and between 6.8 and 8 to form an intermediate phase structure [3]. $\Delta_X < 0.175$ and e/a for BCC crystal structure $1.6 < e/a < 1.8$. For FCC crystal structure $1.8 < e/a < 2.3$ [28].

Several assessments related to the advancements in HEAs are (i) Eliminate the use of a random selection of elements. (ii) Use alloys to reduce or combine enthalpy. (iii) Assessing alloy properties in their original, as-cast state. (iv) Intersection of phase fields in multi-dimensional phase space. The description of the microstructure is incomplete. The description of the solid solution phase is inconsistent [30]. Recently, the addition of MXene as reinforcement has emerged as a potential approach in material science for advancing HEAs alloy systems. Inorganic materials, specifically carbonitride, compose these two-dimensional structures. These structures are thin, have a sheet-like shape, and exhibit varying amounts of bonding. The incorporation of MXene into HEAs for hydrogen storage applications is unique because it significantly enhances two key properties: high surface coverage and high conductivity. MXene is in the form of nanosheets and its stability is limited, so the addition of oxide-based materials is necessary to enhance its stability. The use of layered double hydroxides in MXene production aims to improve both stability and ease of re-stacking. However, the development of HEAs for hydrogen storage relies on the following design requirements.

- Alloy composition or selection
- Fabrication routes – Vacuum arc melting, laser engineered net shaping (LENS), direct laser metal deposition (DLMD), melt spinning (MS) and ball milling then sintering.
- Alloy type – low, medium, and high entropy alloys
- Unit cell volume
- Enthalpy (kJ/mol) and entropy(J/mol-k) formation (ΔH_{form} and ΔS_{form}) for hydrogeneration
- Electronegativity different $\Delta\chi$ in (%) calculated with the help of the Pauling electronegativity scale.
- Valence electron concentration (VEC)
- Enthalpy of mixing (ΔH_{mix})
- Entropy of mixing (ΔS_{mix})
- Inside the pressure (bar) supply at the time of hydrogeneration
- Hydrogeneration temperature T (°C)
- Hydrogen-to-metal ratio (H-M) at supply pressure-temperature conditions.

4.3. Multiple core effects of HEAs

Physical metallurgy is crucial in directing the core effects in HEAs to develop their properties. The principles of crystallography, phase change, thermodynamics, kinetics, mechanical metallurgy, and corrosion science are adopted to incorporate the required properties. The selection of elements is known to have correlations with their behaviour, crystal structure, and the formation of physical and mechanical properties such as strength, fatigue behaviour, toughness, creep, and wear. The configurational entropy changes in the disordered solid solution

Table 1
Various parameters and acceptable values for the formation of a simple disordered phase.

S. No	Parameters	Values
1	Enthalpy of mixing (Hmix)	$-15 \leq$ H mix ≤ 5 kJ/mol
2	Entropy of mixing (Smix)	$12 \leq$ S mix ≤ 17.5 J/(K mol)
3	Atomic size differences (δ)	$\delta \leq 4.3$

Table 2
Various parameters and acceptable values for forming simple and complex ordered phases.

S. No	Parameters	Values
1	Enthalpy of mixing (Hmix)	$-22 \leq$ Hmix ≤ 7 kJ/mol,
2	Entropy of mixing (Smix)	$11 \leq$ Smix ≤ 19.5 J/(K mol)
3	Atomic size differences (δ)	$\delta \leq 8.5$

state of HEAs primarily cause the high entropy effects. Lattice-distortion effects refer to the impact of changes in the arrangement of atoms on a material's mechanical characteristics. Parameters such as the size of the atoms involved determine these changes. Sluggish diffusion effects occur when elements are added to a substance, reducing the diffusion rate. The cocktail effect refers to the phenomenon of non-linear synergy [31]. Fig. 2 **illustrates the core effects of HEAs.**

4.3.1. High entropy effect

This effect is based on natural thermodynamics which, tends to facilitate the formation of solution phases and lead to a significantly simpler microstructure than anticipated in conventional alloys. With this assistance, the formation of the solid solution may increase the level of entropy. Boltzmann notation can be used to predict the level of configurational entropy.

$$S = k \ln(N) \tag{2}$$

From equation (2), S denotes configurational entropy, N = number of elements present, k = Boltzmann constant.

The stability of HEAs is dependent on their entropy levels. Finally, minimizing or lowering Gibbs free energy improves alloy stability. Here, the solid solutions are considered in random and ordered phases. Random phases are short-range in lattices occupied by components. It is expected that BCC, FCC, and occasionally HCP undergo random phase transitions. Ordered phases are distinct constituent elements that occupy a different lattice site. It is expected to have intermetallic phases (IPs) in an orderly or partial-order solid solution [28].

Table 3 and 4 represents the various parameters depending on order and random solid solutions. For that solid solution, there are some important considerations of high entropy effects compared to other effects. The levels of entropy and enthalpy primarily influence the creation of simple solid solution (SS) phases. According to Gibbs's free nature, the addition of elements is more likely to result in a higher amount of entropy and a lower level of enthalpy. Followed by more positive entropy and high chances for the development of intermetallic compounds (see Table 4).

4.3.2. Severe lattice-distortion effect

In HEAs or multi-component alloys, the effects of strains created at the atomic level are the main consequence. Lattice-distortion effects (LDE) clearly explain this behaviour, as the addition of non-symmetric neighbouring atoms causes variations in atomic sizes. The effects of the crystal structure are an important factor in deciding the behaviour of SLD. **The SLD effects of different sizes of elements, bonding natures, and their crystal structure reduce the dislocation movements and are favorable for the formation of solid solution strengthening.** In FCC crystal structure comparisons, adding alloying elements at the same percentage or equi-atomic level results in a lower distortion rate than BCC. Moreover, BCC solid solution structures have a high solution-hardening nature [28].

$$\delta\,(\%) = 100\% \times \sqrt{\sum_{i=1}^{n} c_i \left(1 - \frac{r_i}{\sum_{j=1}^{n} c_j r_j}\right)^2} \tag{3}$$

Table 3
Parameters based on ΔHmix, ΔG, and -TΔS in ordered and random solid solution [28].

Parameters	Compounds	Ordered solid solution	Random solid solution
Mixing enthalpy (ΔH_{mix})	Large negative	Medium negative	Medium negative
Gibbs free energy (ΔG)	Large negative	Large negative	Large negative
-TΔS	Near Zero	< - RTIn(n)	< - RTIn(n)

Table 4
HEAs developed for Hydrogen storage applications.

S.No	Alloys	Fabrication routes	ΔS_{mix}	ΔH_{mix}	V_M	ΔS_{form}	ΔH_{form}	Δ_X	δ	H/M	T	P	VEC	Crystal structure	Ref
1	$Mg_{35}Al_{15}Ti_{25}V_{10}Zn_{15}$	HEMB	12.58	−0.41	16.31	–	–	6.53	9.43	1.00	40	100	4.45	BCC	[32]
2	$Ti_{0.30}V_{0.25}Zr_{0.10}Nb_{0.25}Ta_{0.10}$	AM	12.59	0.00	17.37	–	–	5.65	5.52	2.00	100	33	4.60	BCC	[33]
3	$Al_{0.10}Ti_{0.30}V_{0.25}Zr_{0.10}Nb_{0.25}$	AM	12.59	−8.95	17.12	–	–	5.65	5.45	1.60	25	254.40	4.40	BCC	[34]
4	AlCrFeMnNiW	BM	13.38	−12.5	15.66	–	–	5.82	7.94	0.31	25	0	6.80	BCC	[35]
5	$MgZrTiFe_{0.5}Co_{0.5}Ni_{0.5}$	BM	14.43	−13.8	14.54	–	–	10.70	15.611	0.67	350	20	5.22	BCC	[36]
6	$MgTiNbCr_{0.5}Mn_{0.5}Ni_{0.5}$	HEBM	14.43	1.75	17.44	–	–	8.54	10.94	0.89	100	30	5.00	BCC	[37]
7	HfNbTiVZr	AM	13.38	0.16	19.07	−59.0	−82	7.06	9.33	1.90	290	10	4.40	BCC	[38]
8	$TiVZr_{0.5}NbTa_{0.5}$	AM	12.97	0.03	17.38	–	–	5.94	6.00	1.91	25	20	4.63	BCC	[39]
9	$TiVZrNbHf_{0.5}$	AM	13.15	0.03	18.67	–	–	7.10	8.74	2.00	25	40	4.44	BCC	[40]
10	$TiVZr_{0.5}NbHf$	AM	13.15	0.21	18.36	–	–	6.88	9.07	1.99	25	40	4.44	BCC	[40]
11	$TiV_{0.5}ZrNbHf$	AM	13.15	1.08	19.50	−59.1	−87	6.29	9.28	1.96	25	40	4.33	BCC	[40]
12	TiZrHfMoNb	AM	13.38	−1.58	19.14	–	–	6.09	19.52	1.20	100	5	4.60	BCC	[41]
13	TiVZrNbTa	AM	13.38	0.38	17.94	–	–	6.38	6.93	1.50	25	50	4.60	BCC	[42]
14	$CoFeMnTiVZr_{1.6}$	AM	14.74	−19.4	15.02	–	–	9.93	12.29	1.10	25	100	5.97	C_{14} laves	[43]
15	$CoFeMnTi_{1.5}VZr$	AM	14.78	−18.5	14.43	−29.3	−103	9.02	11.11	1.09	25	100	6.00	C_{14} laves	[43]
16	$CoFeMnTi_{1.5}VZr$	AM	14.78	−18.5	14.53	−29.3	−103	9.02	11.11	1.09	25	100	6.06	C_{14} laves	[43]
17	$CoFeMnTiV_{1.6}Zr$	AM	14.74	−16.8	14.50	−26.9	−100	8.93	10.88	0.93	25	10	6.06	C_{14} laves	[43]
18	$CoFeMnTiVZr_{1.3}$	AM	14.85	−19.1	14.49	–	–	9.65	11.90	1.03	25	100	6.06	C_{14} laves	[43]
19	CrFeMnTiVZr	AM	14.78	−11.1	14.65	–	–	9.04	9.15	1.12	5	25	5.54	C_{14} laves	[44]
20	$Cr_{1.25}FeMnTiVZr$	AM	14.87	−10.7	14.53	–	–	9.29	9.29	0.97	5	25	5.68	C_{14} laves	[45]

Where,

N = Number of various elements.

c_j = Elemental composition of $i^{th}j^{th}$ elements or atomic fraction

r_i, r_j = Atomic radius of $i^{th}j^{th}$ elements

The high degree of natural distortion leads to the development of random solid solutions in HEAs. Distortion and its relaxation are important factors for balancing the elimination or reducing the movement of atoms or misfits within a limit of 6.6%. The negative impact of SLD effects is that the prediction level of local lattice strain or atomic displacements is difficult to measure. They're lowering the intensity levels in XRD. Next, they reduce the electrical and thermal conductive natures and minimize the temperature-dependence properties. The strengthening mechanism concepts ensure that improving the hardness level does not affect the mechanical properties while also lowering the distortion energy due to the maintained atomic stress.

4.3.3. The sluggish-diffusion effect

Sluggish diffusion effects imply a lower kinetic diffusion rate and a phase transformation at slower atom movement. The sluggish diffusion effect results in slower diffusion and higher activation energy during the fluctuating migration of atoms. The most challenging task for evaluation is finding the diffusion in the addition of more than three elements. The seven-bond interaction energy explains the slow diffusion nature. It represents energy distribution through sluggish diffusion effects. Diffusion measurement in HEAs is based on the diffusion coefficient (temperature-dependent T/Tm) and activation energies (Q/Qm) [31]. Recent HEAs studies are considered to minimize the diffusion rate in alloy systems, followed by the diffusion coefficient and inter-diffusion coefficient [46]. An emerging role in the field of entropy generation is based on their diffusion kinetics, with the help of an evaluation of chemical and atomic size mismatches [47]. The FCC structure has very little sluggish diffusion compared to other crystal structures. The diffusion behaviour of the $Co_{20}Cr_{20}Fe_{20}Ni_{20}Mn_{20}$ HEAs, when annealed at different temperature ranges such as 900 °C, 1000 °C, 1100 °C, and 1200 °C, differs significantly from the conventional alloy system $Al_{48}Ni_{52}$ [48].

4.3.4. Cocktail effect

The effect clearly expresses unexpected synergies due to the addition of various elements. These effects determine the interrelationships between strength, plasticity, and coercivity. The segregation of elements, grain accumulations, grain boundaries, and morphology variations at the time of alloying addition directly relate to strength and plasticity, while electrical applications primarily use the term coercivity [8]. Refractory-based HEAs in high-temperature applications mostly use this effect [49].

4.4. Phase stability of HEAs

Phase stability of the alloy system is an important factor for improving the alloy stability in all environmental conditions. The phase stability depends on the addition of alloying element selection. In this way, the entropy stabilizes the phase structure and mechanical properties of the alloy system. In hydrogen storage equipment one of the reasons for developing failure inside the materials is the change in crystal structure due to hydrogen exposure, followed by, phase stability losses due to hydrogen-induced conditions. Phase stability losses are eliminated with the help of improving the entropy level by the addition of alloying elements. That is the correlation between HEAs and hydrogen storage-related studies. Adding multiple elements to enhance the individual entropy level of the alloy system is a simple understanding of HEAs development.

The phase stability of HEAs depends on the incorporation of entropy and enthalpy formation. Thermodynamics and Gibbs free energy govern these processes. Recently, researchers have focused on HEAs with the alloy addition over equi-atomic and non-equi-atomic composition in various element additions [48]. The lowest Gibbs free energy is not necessarily advantageous for developing high entropy. This outcome also relies on thermodynamic factors [50]. The transition metal group has undergone higher entropy stabilization in recent decades than other element groups. Obtaining a single phase in HEAs is crucial due to criteria such as BCC, FCC, and HCP, and there has also been significant research on intermetallic. Many factors contribute to achieving that single phase, including the selection of elements, atomic size, VEC, H formation, and S formation.

At elevated temperature conditions, entropy plays a vital role compared to enthalpy for better stability [30]. Table 4 shows the list of HEAs developed for hydrogen storage systems and the quantitative values of the parameters such as ΔS_{mix} [J/mol-K] = **Entropy of mixing,** ΔH_{mix} [kJ/mol] Enthalpy of mixing, V_M [$Å^3$] = Unit cell volume per one averaged metal atom, ΔS_{form} [J/mol-K] Entropy of hydrogeneration, ΔH_{form} [kJ/mol] = Enthalpy of hydrogeneration, Δ_X [%] = Electronegativity mismatch, δ [%] = Atomic size different, H/M = Hydrogen-to-Metal ratio, T = Temperature, P = Pressure, VEC= Valency Electron Concentration. HEBM = High Energy Ball Milling, AM = Arc Melting, **BM= Ball Milling.**

5. Hydrogen absorption behaviour in HEAs

In energy-transparent applications, the flow of hydrogen inside the materials absorbs the hydrogen at a certain level based on the alloy composition. After entering metals, hydrogen gathers in voids and becomes trapped at internal interfaces, dislocations, and vacancies. The formation of lattice defects influences the physical, chemical, and mechanical properties. Once hydrogen enters the sites, it enhances localized plasticity, decohesion, metal hydride, or void coalescence [51]. In an alloy system, hydrogen absorption deviates from Sievert's law. In the presence of hydrogen atoms, a higher amount of hydrogen absorbs the materials, reducing their mechanical properties, such as toughness or ductility. The PCT curves explain the absorption of hydrogen in the different alloy systems. The solubility of hydrogen among the elements increases, and the hydrogen absorption rate decreases, and vice versa. The alloying system, undergoing high elastic deformation, requires a higher amount of hydrogen to absorb [52].

6. Hydrogen embrittlement mechanisms

Hydrogen-induced materials are affected by HE-related failures. HE mechanisms include Hydrogen-Enhanced De-cohesion Mechanism (HEDE) [53], Hydrogen-Enhanced Local Plasticity (HELP) model, Adsorption-Induced Dislocation Emission (AIDE), Hydrogen-Enhanced Macroscopic Ductility (HEMD), Hydrogen-Changed Micro-Fracture Mode (HAM), Decohesive Hydrogen Fracture (DHF), Mixed Fracture (MF), Hydrogen Assisted Micro Void Coalescence (HDMC) [54,55]. The individual and combined effects of theses mechanisms are responsible for HE and its mechanical degradation behaviour.

6.1. Hydrogen-enhanced de-cohesion mechanism (HEDE)

Hydrogen may directly weaken the atomic bonds that hold the metal lattice together, leading to a brittle fracture and failure in the intergranular form. There isn't enough hydrogen soluble in metals to cause a noticeable de-cohesion effect, but the strength of the atomic bond strongly correlates with the interatomic-repulsive forces. To minimize the interatomic repulsive force, the atomic bond strength is to be increased. Fig. 3 (a – c) explains the effect of hydrogen inside the lattice.

The introduction of hydrogen into flow channels near the crack tip leads to the accumulation of hydrogen atoms in that particular area. The concentration of hydrogen atoms reduces the impact of interatomic bond strength. The accumulation of atoms in this particular type of material leads to stress formation as a result of diffusion, which

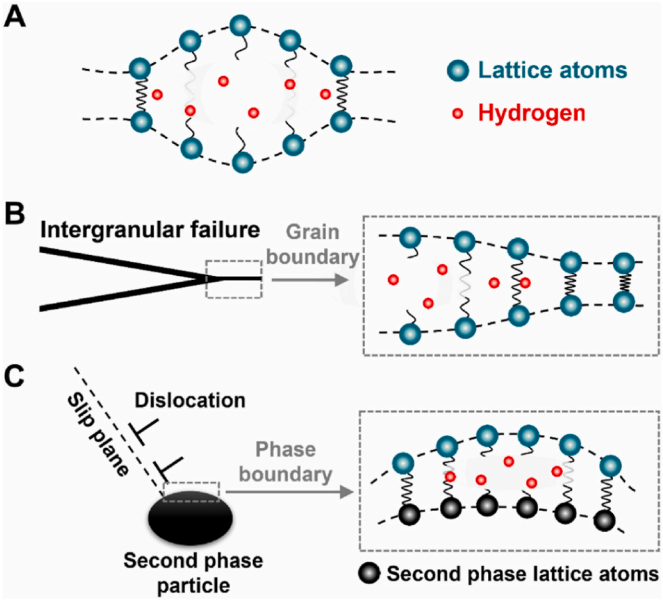

Fig. 3. (A) Effect of hydrogen inside the atoms surrounded by the lattice atoms. (B) The influence of the hydrogen atoms that develop intergranular failure inside the materials. (C) Effect of hydrogen in primary and secondary phase lattice atoms [56]. Open access article, which permits unrestricted use.

subsequently causes a decrease in the cohesive or interatomic strength [53]. The cohesive strength of a material is strongly correlated with its surface energy. By decreasing the surface energy of the materials, the cohesive force is also reduced, which can lead to the formation of a fracture resembling cleavage [53].

6.2. Hydrogen-enhanced local plasticity (HELP)

Dislocation motion plays a major role in HELP mechanisms. When hydrogen flows in an energy-transparent medium such as a pipe, it accumulates near the crack tip, reducing the dislocation motion. Consequently, the dislocation motion's mobility increases. The interesting theory about HELP has (I) high tensile hydrostatic stress developed with the help of interstitial hydrogen atoms. (II) Hydrogen located inside the lattice has a high chance of segregating and is made of dislocations [57], which results in plastic deformation on a lattice plane [58].

Fig. 4 explains the various zones of the HELP mechanism with the zone (I, II) high hydrostatic stress zone with hydrogen concentration in the Cottrell atmosphere that reduces the strain energy and controls the dislocation motions. Zone (III) indicates that the strain-induced microvoids are reduced from crack propagation to failure zone. Zone (IV) indicates the effects of less strain localization (without hydrogen) which

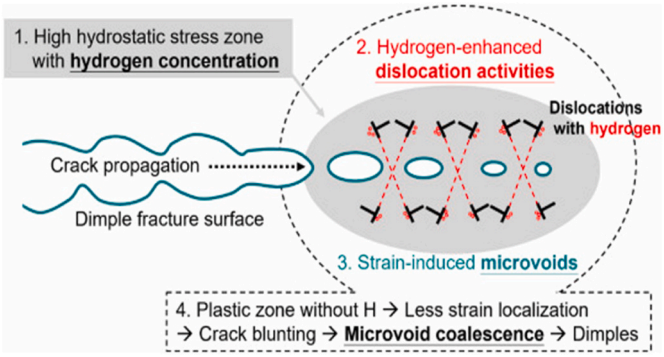

Fig. 4. The effects of HELP mechanism and their behaviour at various zones [56]. Open access article, which permits unrestricted use.

supports crack blunting and reduces the microvoid formations [56]. Hydrogen concentration at the crack tip mostly depends on the type of fracture, such as *trans*-granular, intergranular, or quasi-cleavage. Because of this, fractography analysis shows that the crack tip region has less ductility and more plastic deformation. The hydrogen atom has the effect of reducing both the activation energy and activation area for dislocation motion [59,60].

6.3. Adsorption-Induced Dislocation Emission (AIDE)

The AIDE mechanisms function with de-cohesion and dislocation in the crack tip. Hydrogen flows through the channels or pipeline, and the hydrogen-transparent materials absorb the solute hydrogen atoms, developing an internal stress concentration and a micro void formation. Fig. 5 explains that the dislocation movement facilitated by surface adsorption of hydrogen causes the dislocation to originate from the surface and develop an inward strain. The development of microvoids close to the plastic zone leads to plastic zone coalescence, which propagates cracks and forms a dimpled fracture surface.

HEDE is concerned with hydrogen adsorption, which reduces interatomic bonding. HELP deals with dislocation motion at the crack tip, which develops crack growth and the formation of micro-voids. AIDE deals with de-cohesion and dislocation emissions at the crack tip that has caused nucleation and fracture development in a region. Elements like Ni, Ti, and Fe adsorbed a higher amount of hydrogen at the material surface [61,62].

6.4. Hydride-formation

Hydride formation happens in an alloy system when hydrogen atoms combine with the metal, forming compounds known as hydrides. Most of the time, this process forms brittle hydrides. They are from cleavage fractures. Specific materials like Ti, Zr, Ni, V, Mg, and Ta are mostly supporting elements for hydride formation. Hydrides are classified into two categories: those that are thermodynamically stable and those that induce stress. Metals and their alloys combine thermodynamically stable hydrides with high hydrogen concentrations without taking stress into account. Stress-induced hydrides have lower hydrogen concentrations, followed by high-applied stress [63]. When the local hydrogen concentration gets close to or above the material's solubility limit or when the mutual solubility ranges are exceeded because of the alloying elements, hydrides form. There are more chances to form a metal hydride. To achieve this, alloy systems use non-isotropic crystal structures to form a hydride. The non-isotropic crystal structure is more resistant to the formation of HE. Fig. 6(A) explains the metal lattices; hydrogen enters in the form of foreign interstitial atoms, diffuse and moderately segregated to develop hydrostatic stress in the crack tip.

Fig. 6(B) shows brittle hydride formation with the addition of hydride-forming elements Ti, Zr, Mg, etc, exceeding the solubility limit. Fig. 6(C) shows that, with the help of hydride formation, crack is arrested. The alloying addition of Ni or Fe are non-hydride forming elements [56].

6.5. Other mechanisms

Hydrogen-enhanced macroscopic plasticity **(HEMP)** mechanism is the one in which high-strength materials like steel are influenced by the hydrogen atoms in the material, reducing its yield strength. Hydrogen diffusion causes the material to soften in a solid solution. The term macroscopic enrichment plasticity refers to the material yielding and plasticization in the entire volume to occur [64,65]. Hydrogen-changed micro-fracture mode **(HAM)** is another mechanism that explains how material crystal structure changes as a result of hydrogen charging. For instance, the transition from ductile to brittle occurs due to the effects of hydrogen uptake, which is then advantageous for cup and cone brittle fracture [66]. Decohesive hydrogen fracture **(DHF)** is the process in

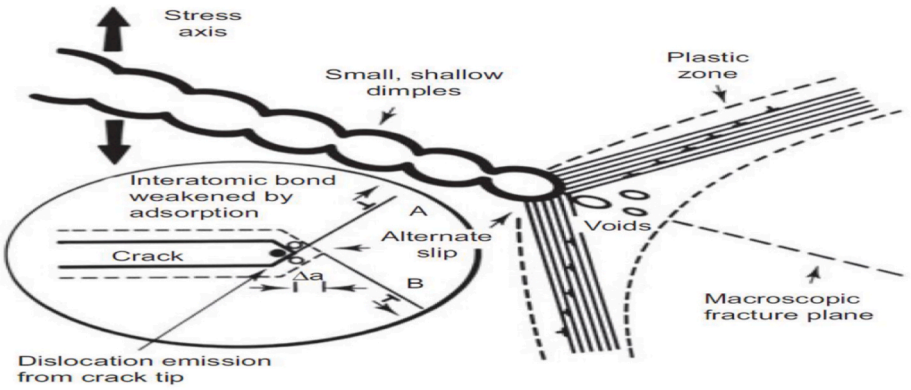

Fig. 5. Schematic view of the AIDE mechanism and the hydrogen-induced condition [59]. Reuse with journal permission. Copyrights 2024, Elsevier.

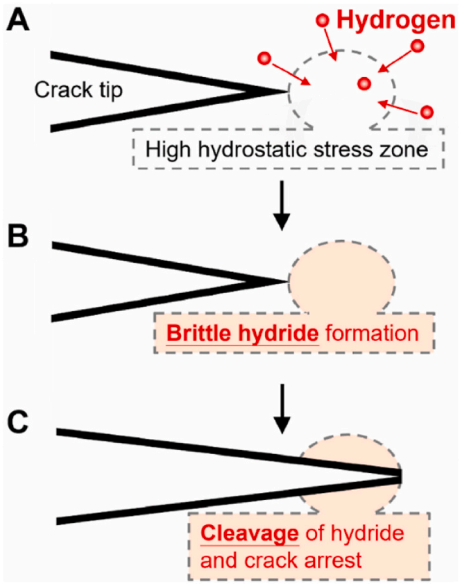

Fig. 6. Schematic diagram of HIC for the formation of brittle hydride to arrest the crack [56]. Open access article, which permits unrestricted use.

which the ductile fracture is initiated by the brittle nature of the sample with the help of de-cohesion or hydrogen in nature. Mixed fracture **(MF)** mode is the condition in which the fractured surfaces are visible to address fractures that are both ductile and brittle or have a combined effect. In hydrogen-assisted micro void coalescence **(HDMC)** mode, ductile fracture in a material took the form of micro-void coalescence. There were several stages of the MVC fracture: void nucleation, void development, void coalescence, crack extension, and shearing off of the remaining ligament. The convergence of voids in the fracture propagation direction caused the cracks to expand in a zigzag pattern. Hydrogen impact results in dislocation motion and localized plastic deformation in a material [67].

7. Hydrogen embrittlement assessments on HEAs

The development of HEAs is the most promising and successful way to fulfil the materials requirements for hydrogen storage applications. Following material development and fabrication of samples, the next important thing is material characterization based on ASTM standards. Different characterization methods include mechanical testing, hydrogen permeation testing, hydrogen uptake measurements, thermal desorption spectroscopy (TDS), hydrogen diffusion analysis, and environmental exposure testing. Hydrogen atoms travel very quickly within a substance due to their small size. The techniques used for characterization include atom probe tomography (APT) to investigate the nanoscale distribution of hydrogen in the materials [68]. A secondary ion mass spectroscopy (SIMS) analysis of hydrogen behaviour characterization at the microscale level can also predict how the alloy will separate inside. The interfaces of Fe–Al, Ti–Al, and Ti–Al–V are examples of this [69]. The average hydrogen concentration in alloying elements can be investigated using the glycerine method and found that increasing the hydrogen concentration in alloying samples directly increases the hydrogen charge current density. The limitations include material embrittlement, reduced fracture toughness, and increased fatigue crack growth [70]. The inert gas fusion heat conduction method (IGFHCM) and thermal desorption spectroscopy (TDS) find the hydrogen desorption rate in the sample. TDS techniques were applied to determine the activation energy for various hydrogen trap locations. Hydrogen micro-print techniques (HMT) are another important way to characterize hydrogen because they look at how changes in the microstructure of the pipes affect the flow of hydrogen [71].

7.1. Mechanical testing (tensile test)

Tensile tests are the most common method for evaluating HE on materials. The performance of the high-entropy alloys (HEAs) is evaluated under two conditions: with and without hydrogen supply. The objective is to identify important mechanical parameters such as elongation, yield strength, and ultimate tensile strength. During the tensile test, the presence of hydrogen in the samples often decreases both the ductility and strength. Additionally, it influences the hydrogen embrittlement which can be evaluated by estimating the index of loss in ductility and strength.

$$\text{Strength loss index} = \frac{\sigma_{ref} - \sigma_H}{\sigma_{ref}} \tag{4}$$

$$\text{Ductility loss index} = \frac{RA_{ref} - RA_H}{RA_{ref}} \tag{5}$$

Here, σ_H and RA_H indicates strength in hydrogen-induced conditions, and σ_{ref} and RA_{ref} Indicates strength in hydrogen-free conditions. Equations (4) and (5) explain the σ_H (loss of strength) and RA_H (loss of ductility) in hydrogen-induced conditions. The ductility and strength loss index indicates % of HE susceptibility to the alloy system to the influence of hydrogen atom attack. The percentage of ductility loss is measured with the help of elongation to fracture and reduction area (RA) [72].

Engineering stress-strain values of CoCrFeMnNi-based HEA is compared with AISI 304 and AISI 316L with and without hydrogen charging conditions [73]. It was found that the precipitation formed by the alloys acts as a barrier to dislocation motion and is highly effective in

reducing the HE in alloy systems. Fig. 7 (a) shows that, compared to austenitic stainless steel (AISI 304 and AISI 316L) samples, HEAs have better HE resistance. Since the stainless-steel samples have to absorb a greater amount of hydrogen compared to HEA, the ductility loss is high compared to HEAs. HEAs undergo fewer ductility losses and high-desorbed hydrogen which supports the resistivity to HE. Fig. 7 (b & c) represents the SEM fractography of CoCrFeMnNi-based HEAs without hydrogen charging and with hydrogen charge respectively. Precipitation-strengthened $(FeCoNi)_{86}Al_7Ti_7$-based HEAs were used to investigate the influence of hydrogen, its HE behaviour, cracking mechanisms, and deformation behaviour in both hydrogen-doped and non-doped samples. When these precipitations are used in energy storage, they can help avoid or control the dislocation density and improve the strength-to-ductility ratio. However, they can also absorb a lot of hydrogen, which can damage the crystal structure. Fig. 8(a–b) shows tensile results of $(FeCoNi)_{86}Al_7Ti_7$ based HEA in various stress and strain conditions. The UTS and % of elongation rate are evaluated with and without hydrogen supply. HEAs subjected to hydrogen supply have high UTS, and fewer elongation losses when compared to the samples without hydrogen exposure.

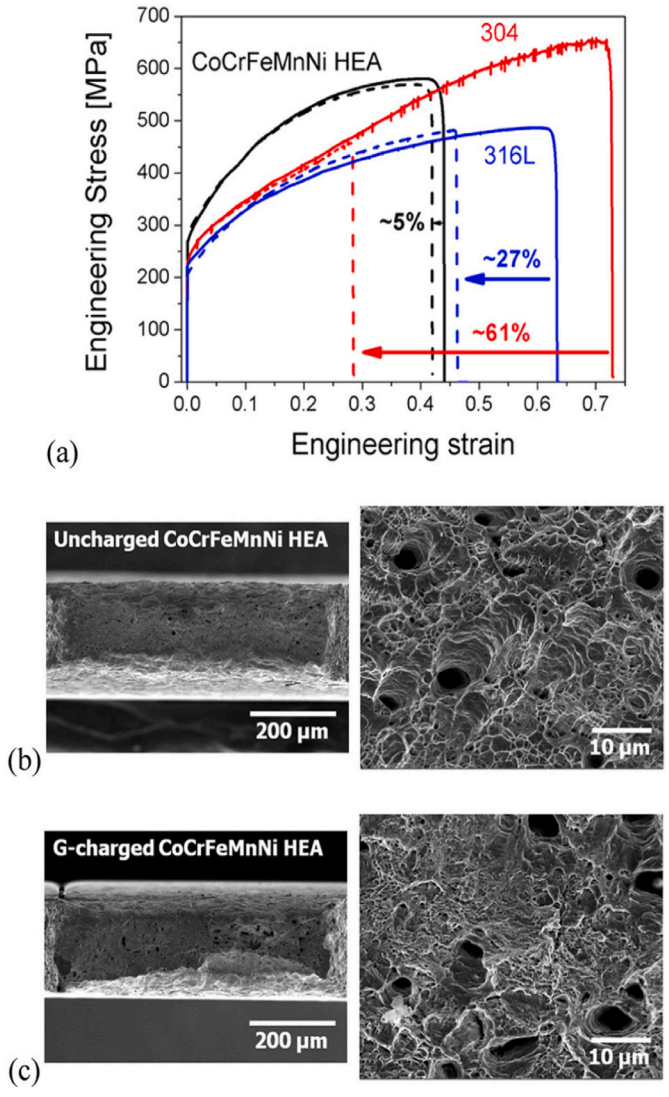

Fig. 7. (a) Tensile test results of hydrogen-doped samples of CoCrFeMnNi-based HEAs compared to AISI 304, and AISI 316L under stress-strain conditions. (b) SEM Fractography of CoCrFeMnNi-based HEAs without hydrogen charging and (c) SEM Fractography of CoCrFeMnNi-based HEAs with hydrogen charge [73]. Reuse with journal permission. Copyrights 2024, Elsevier.

UTS and % of elongation for the samples without hydrogen exposure are 1324.2 ± 16.6 MPa and 35.5 ± 1.1% whereas for the samples with hydrogen exposure are 1351.1 ± 34.6 MPa and 29.6 ± 2.8%. It was found that the effect of hydrogen exposure has improved the UTS and reduced the % of elongation [74]. Another possible way to improve the mechanical properties and resistance to HE is through the grain refinement effect with a high strength-to-elongation balance. HEAs made of CoCrFeMnNi with 1.9 μm grain size were reformed and improved with the help of a thermomechanical process. A comparative study based on coarse and fine-grain refinement effects on HE evaluation was reported. Fig. 9 explains the performance of the HEAs with and without hydrogen supply for fine (FG), and coarse grain (CG) heat-treated samples.

That stress-strain rate explains the degradation of mechanical properties based on the exposure to the hydrogen (with and without hydrogen supply). While comparing the tensile strength results of the FG800 and CG800, the FG800 has shown an improvement in strength because of its lower hydrogen uptake. The strength of FG800 is 1.5 times higher compared to CG800. However, the samples with FG700 have more strength compared to the FG800 and CG800. The results indicate that grain refinement is an important consideration for preventing HE [75].

7.2. Thermal desorption analysis based on hydrogen trapping

Hydrogen permeation tests and thermal desorption analysis (TDS) are hydrogen trapping (HT) evaluation processes. The HT is an intrinsic approach that introduces microstructure changes as hydrogen is added to the alloying system. The extrinsic approach involves a metal surface coating. In HT, the uniform hydrogen concentration leads to an increase in the solubility limit of hydrogen throughout the alloy system, as explained in the HT principles: (I) activation energy is one of the influencing factors for reduction of hydrogen accumulation in the lattice site; (II) migration of the trapping site depends on activation energy; (III) de-trapping energy required for trapped hydrogen atoms to diffuse the lattice; (IV) binding nature of the trapping site [76].

Fig. 10 explains the working principle of Thermal Desorption Analysis (TDA). Bulk samples were placed over the furnace and hydrogen was charged at the inlet. The sample absorbed the excess hydrogen in the form of desorbed hydrogen. The vacuum pump and gas detector desorbed the hydrogen gas. After collecting a sample from the furnace, the hydrogen desorption rate between the various temperatures is evaluated with the help of hydrogen desorption peaks.

8. Taming the hydrogen threat: strategies to prevent the hydrogen embrittlement in high-entropy alloys (HEAs)

8.1. Hydrogen embrittlement

Maintaining a green environment is challenging for society as a whole. Moreover, the CO_2 level has increased because of the increased human population, transport sectors, energy demand, and deforestation. Consequently, current research primarily concentrates on utilising sustainable energy sources, including hydrogen. The synthesis of hydrogen generation, storage, and transport is a complex endeavour because of the storage container's inherent vulnerability to chemical degradation. Mechanical properties degrade, causing the material to fail [77]. The safe handling of hydrogen is crucial. When the concentration of hydrogen in the air exceeds the lower explosive limit, it becomes combustible and requires careful handling. In that situation, increasing the credibility of hydrogen among the people is an important consideration in developing hydrogen-based vehicles for society. The Australian National Survey Institute conducted a hydrogen-related safety survey, providing results on a 5-point scale and four significant factors based on customers' willingness to use hydrogen. Safety-related ratings are 4.5/5, reliability 4.3/5, convenience to use 3.6/5, and economic cost

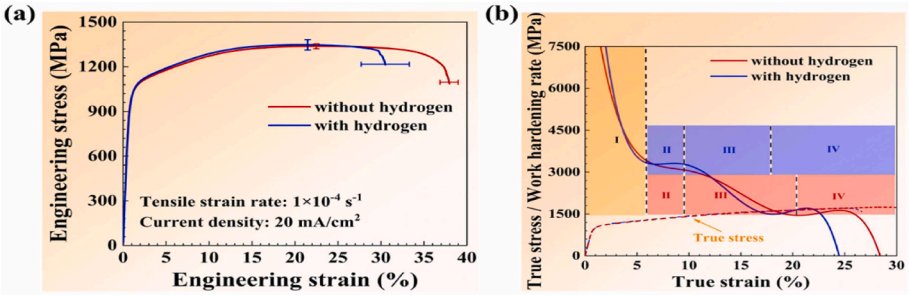

Fig. 8. (a) Engineering stress and strain results with hydrogen and without hydrogen supply (b) True stress and true strain illustrations of work hardening rate with and without hydrogen supply. Reuse with journal permission. Copyrights 2024, Elsevier.

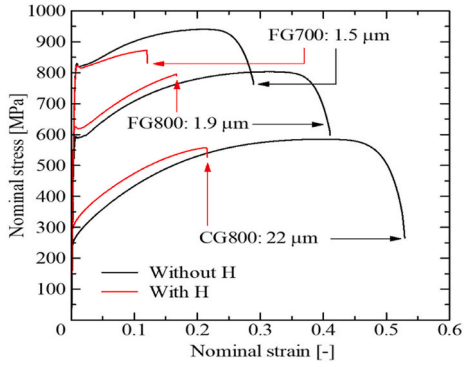

Fig. 9. Effect of fine and coarse grain refinement in CoCrFeMnNi-based HEAs and their stress-strain curves [75]. Reuse with journal permission. Copyrights 2024, Elsevier.

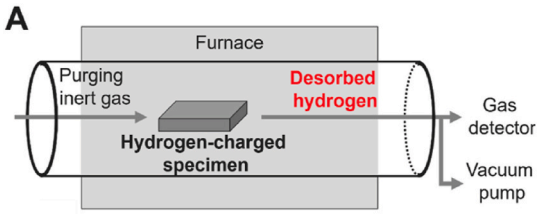

Fig. 10. Thermal desorption analysis model [56]. Open access article, which permits unrestricted use.

4.2/5 [56]. The mechanism of HE and the analysis of microstructure are important for the evaluation of HE formation and its prevention methods. There are two different forms of HE in materials (a) internal hydrogen implantation (IHE). Remaining hydrogen from production and processing techniques triggers the IHE, or industrial hydrogen embrittlement, which leads to the accumulation of hydrogen in the crack tip through diffusion from the crystal lattice. (b) External Hydrogen Embrittlement (EHE). The term EHE refers to the influx of hydrogen from outside sources, such as environments that are rich in hydrogen, and causes the materials for hydrogen adsorption, diffusion, and decomposition. EHE is an example of the stress corrosion cracking factor [78]. Many factors contribute to the HE in materials namely, selection of alloying elements, (ii) microstructure, (iii) stress development over the materials, (iv) hydrogen content, (v) stress and strain ratios, (vi) temperature, (vii) surface condition, and (viii) percentage of hydrogen purity level [23]. Fe-based alloys are more likely to be affected by HE due to their higher penetrating level of hydrogen (<1 ppm) and high strength in nature. The following criteria are to be considered to strike a balance between the mechanical properties (strength, corrosion, material ductility) of the developed material and HE: (i) Inadequate hydrogen diffusivity and the absence of gradients in the local electrochemical process contribute to the development of these mechanical properties. ii) When testing for slow strain rate tensile, the solute hydrogen in the bulk alloy matrix creates deformation twins that stop cracks from spreading. (iii) To control hydrogen uptake and minimize the formation of defects, such as point defects, oxide-based films are applied over the surface [79]. Hydrogen diffusion and hydrogen characterization are important methods for the evaluation of HE [78]. Mechanical failure, such as fractures (intergranular and transgranular) is a significant factor in HE failure. These types of fractures are caused by hydrogen's ease of trapping in metals. The presence of HE in a material is determined not only by its natural trapping, but also by factors such as temperature, pressure, alloying element addition, material strength, stress, and strain rate, microstructure, internal surface conditions, heat treatment, and working nature [80]. HE is categorized as a catastrophic failure due to the loss of mechanical parameters such as toughness, ductility, and strength, as well as the propagation of subcritical cracks and fracture initiation. At fracture initiation, the stress level is between yield and ultimate tensile strength levels. In comparison to other alloying systems, HEAs are highly resistant to HE because the influence of a single alloying system doesn't influence the mechanical properties of HEAs. Various alloying additions enhance the resistance to hydrogen evaporation (HE_V). These days, a highly effective method for storing hydrogen is in metal-based tanks that can withstand high pressure or low temperature. In this way, HEAs are more effective at resisting HE. HE is evaluated using the embrittlement index (E1) and determines the hydrogen-induced ductility loss.

$$E_1 = \frac{Eh\ (air) - Eh(\ hydrogen)}{Eh\ (air)} \times 100\ \% \tag{7}$$

E_h: homogeneous deformation.

The investigation of CoCrFeMnNi-based HEAs is focused on the effect of temperature ranges like 298 K, 177 K and 77 K. For the 177 K range, a higher number of twins forms, which improves hydrogen diffusion and minimizes stress concentration at boundaries. Moreover, further reduction in temperature to cryogenic conditions (77 K) HE issues are not visible to address. Fig. 11 shows that with and without the supply of hydrogen at various temperature limits, materials do not get affected by the HE problem because, at that particular temperature, more deformation twins are present in the microstructure. For the temperature of 77K, it was noted that there is an increase in the strain or elongation level for a decrease in the temperature limits [81]. A kernel average misorientation map (KAM map) is used in Fig. 12 which shows the effects of elongation in a hydrogen-absorbed CoCrFeMnNi-based alloy. Fig. 12(a–f) displays the EBSD results for a sample that did not have a hydrogen supply. The red and black lines show the boundaries of the deformation twins and the high-angle grain boundaries. The deformation twin boundaries highly elongated during the tensile test in the tensile direction at a temperature range of 298 to 77 K. Compared to this limit, 77 K has high deformation. This is primarily due to the high twin length per unit area. Fig. 12 (g to l) shows that the hydrogen supply sample at 77 K has more deformation compared to 298 and 177 K. The

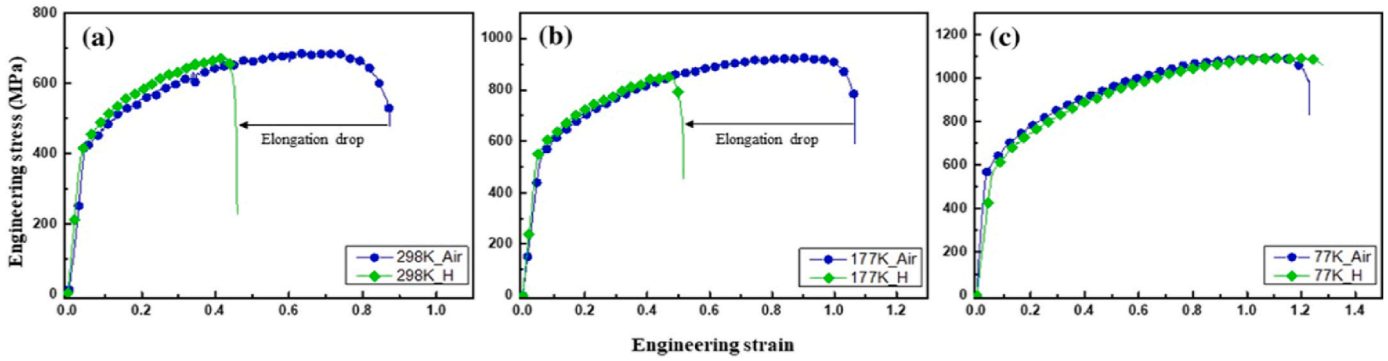

Fig. 11. Effects of stress-strain variation between the various temperature limits (a) 298 K (b) 177 K (C) 77 K [81].

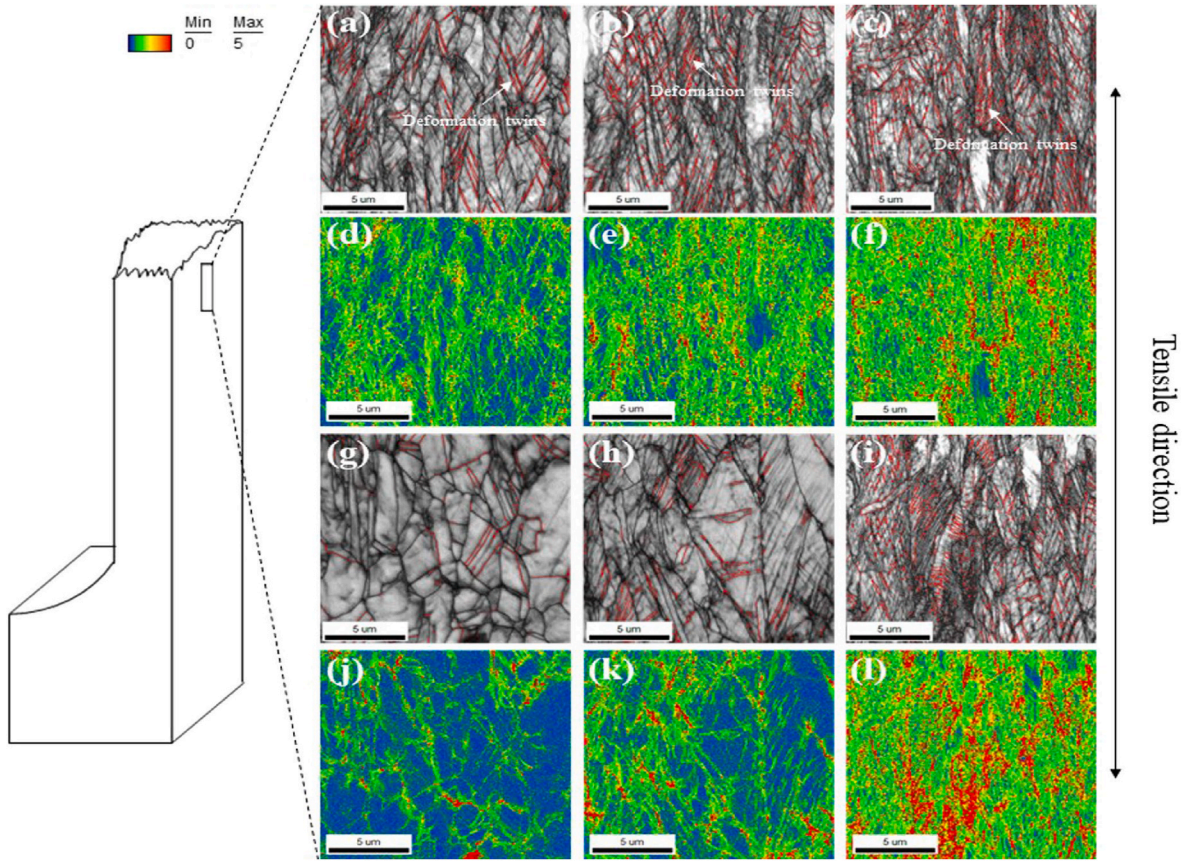

Fig. 12. (a)–(f) EBSD results for a sample without hydrogen supply and (g) to (i) EBSD results for a sample with hydrogen supply at the same temperatures (298 K, 177 K, and 77 K) [81].

blue colour denotes less deformation and fewer deformation twins, which concludes that the high temperature causes more deformation and less possibility for HE [81].

Factors which influence the HE are listed below [82].

- Flow of hydrogen – external (gaseous form) and internal (dissolved form)
- Exposures time
- Pressure and temperature in various conditions
- Effects of solvents (acidic solution)
- quantity of metal discontinuities.
- Handling of exposed panels or surfaces (Barrier coating)
- Treatment of metal surface
- Heat treatment effects

8.2. Prevention of hydrogen embrittlement using HEAs

In hydrogen embrittlement, a mechanical property degradation phenomenon commonly known as hydrogen-assisted cracking (HAC) occurs. Hydrogen-induced-phase transition is one of the effects of HAC on the trapping of activation energy for hydrogen. Crack-tip failure constantly occurs during the HAC phenomenon, followed by continuous and multiple crack growth caused by the influence of hydrogen. The addition of alloying elements, microstructure modification, and oxide films over the surface are the possible solutions to prevent continuous failure in materials. The goal of using oxide films is to reduce hydrogen uptake. For liquid-hydrogen transportation sectors, for high safety and critical fracture, strong and ductile materials are mostly recommended [83]. In recent years, advanced material development sectors have made use of high-strength materials like nickel-based Inconel alloys and

superalloys, titanium-based alloys, aluminium, and stainless steels [84]. These alloy systems are high-strength and have better corrosion resistance, but their limitations are a very small amount of prevention of hydrogen embrittlement due to this microstructure constraint. To rectify these issues entropy-based alloys were developed. One of the best things about some HEAs is that they make it easy to change the microstructure by adding different alloying elements that can be equal or unequal in number. The addition of alloying elements such as Cu, Ni, Co, Cr, Nb, Mo, Ti, Mn, Al, and microalloying elements makes it highly resistant to hydrogen embrittlement. Based on a selection of alloying elements in HEAs, microstructure changes are possible and improve the strength of the alloy system, e.g., This is because the microstructure changes that make the material stronger—interfaces and second-phase precipitates, which cause galvanic corrosion—cause changes in the electrochemical potential that are only localized. In the same way, hydrogen builds up at interfaces, inside precipitates, and in places with a lot of micro-mechanical contrast. This makes the material soften more quickly [85, 86]. The addition of alloying elements concept was used to develop CoNiV-based entropy alloys with FCC structure at a strain rate of 10^{-4} S^{-1}. CoNiV-based alloys work better mechanically in hydrogen environments, don't become weaker when exposed to hydrogen, and resist corrosion well at 300K in a range of acidic environments. Fig. 13 (a) shows the tensile behaviour of CoNiV alloys with and without hydrogen charge. The UTS without hydrogen samples was 1095 ± 10 MPa, with an elongation of 85.8 ± 2.0%. Samples with hydrogen exposure resulted in a UTS of 1079 ± 12 MPa and elongation of 84.3 ± 1.5%. Fig. 13 (b) indicates the hydrogen desorption rate based on TDS curves for hydrogen with and without charge. Fig. 13(c) presents a comparative study of the diffusivity of hydrogen in individual elements such as Co, Ni, and V, as well as in the combined form of CoNiV. The comparison of individual elements reveals that the CoNiV-based alloys exhibit a higher amount of hydrogen diffusivity. Fig. 13(d–h) shows the fracture surface of the hydrogen-charged sample [83]. As the alloying elements $(Nb_{40}\text{-}xMox)_{40}Ti_{30}Ni_{30}$ (X = 0, 5, 10) are added, the level of hydrogen absorption has to go down, and the solubility has to go down as well. In an alloy system, the addition of Mo to other elements has high diffusivity in nature and is highly effective for HE [52].

The addition of alloying and micro alloying elements like Cu, Ni, Co, Cr, Nb, Mo, Ti, Mn, and Al makes hydrogen embrittlement highly resistant. The addition of copper (Cu) to the high-strength steel has good resistance to HE. In general, high-strength materials have very little hydrogen resistance and are more susceptible to hydrogen embrittlement. But, the addition of Cu improves the resistance to hydrogen embrittlement [87]. The electrochemical hydrogen permeation test identifies the effect of copper addition and its influence, while the slow strain rate test scrutinizes its influence in the alloy system. Adding copper to the alloying system makes the other elements more uniform and slowly lowers the buildup of hydrogen because the different elements are pushed down [88]. The alloying elements benefit greatly from the addition of copper. Cu has a very good precipitation former for that effect strength versus HE resistance trade-off, but the advantages do not affect the UTS of core material properties. Moreover, the addition of copper to the alloying process easily forms the oxide layer and reduces hydrogen penetration on the surface [89]. Adding Pd-based alloys to HE works very well because they don't let too much hydrogen through, last longer, bind hydrogen very well, and can be used to have strong catalytic properties on their surfaces [90]. The inclusion of Al in the alloy system raises the stacking fault energy (SFE) which is the primary reason for using Al-based HEAs as the most advantageous ones for HE reduction. High SFE strengthens the barrier against hydrogen-induced delayed cracking (HE) [91]. Therefore it is preferred to increase the SFE to increase the isotropic hardening and reduce the kinetic hardening behaviour in the dislocation pile-up mechanism [89]. In energy-based sectors, the density of materials has played a major role in effective

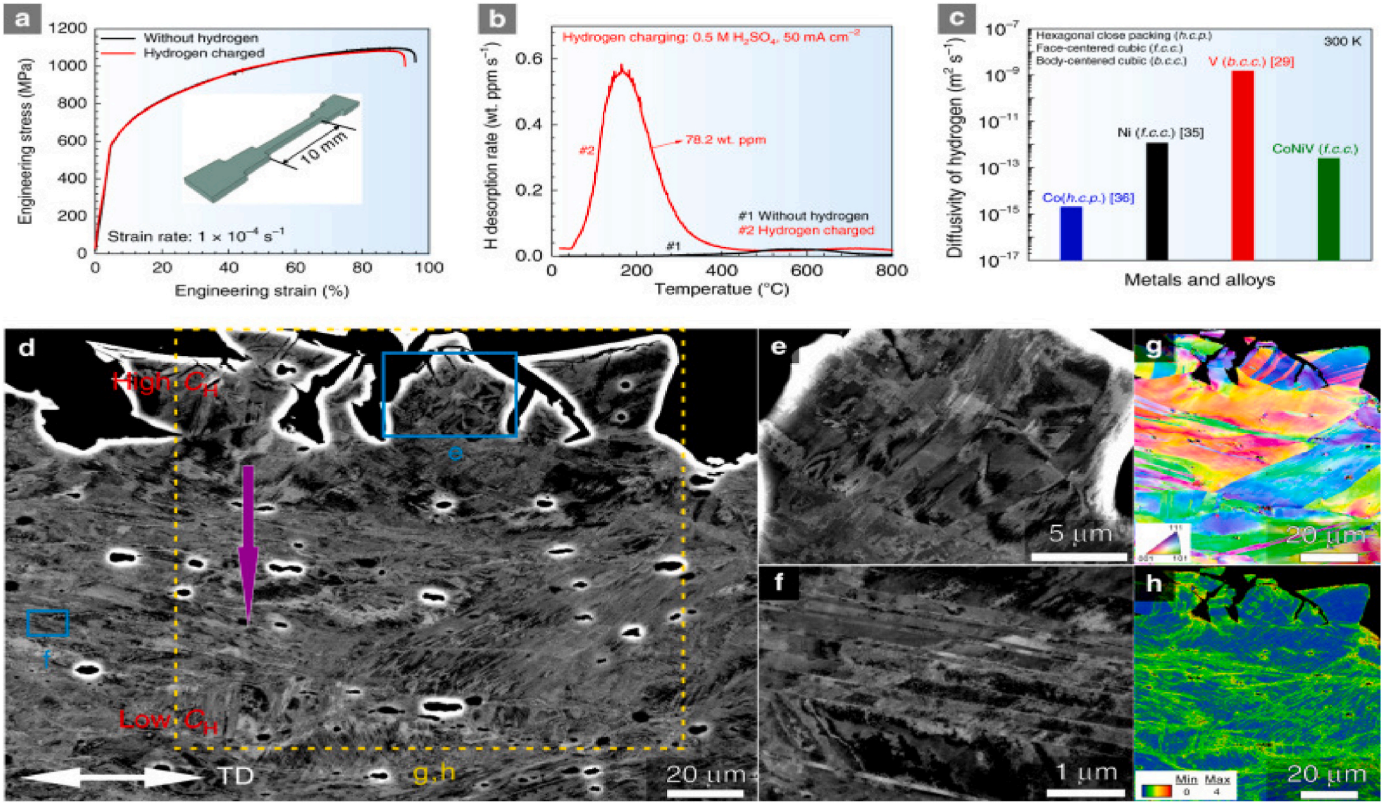

Fig. 13. (a) Mechanical behaviour of CoNiV-based alloys with and without hydrogen charging. (b) Effect of various temperature and its influence factors for hydrogen desorption rate in CoNiV-based alloys. (c) hydrogen diffusivity compared to individual and alloying elements. (d–h) Hydrogen-charged sample and its fracture surface [83]. Open access article, which permits unrestricted use.

energy consumption based on the development of lightweight materials. The addition of Mg to other elements has reduced the density of HEAs and is more favorable for the fabrication of lightweight hydrogen storage applications based on HEAs concepts. In HEAs, the addition of Mg to other elements increases the gravimetric hydrogen storage capacity. Magnesium is a great option for hydrogen applications due to its high gravimetric capacity, high abundance, and affordable cost. High-energy ball milling (HEBM) forms the alloy system of $Mg_{12}Al_{11}Ti_{35}Mn_{11}Nb_{33}$, which absorbs hydrogen at 1.7 wt% and forms the BCC crystal structure with a hydrogen-to-metal ratio of one (H/M = 1). Another HEAs, namely $MgZrTiFe_{0.5}Co_{0.5}Ni_{0.5}$ developed using HEBM, absorbed hydrogen at a rate of 1.2 wt% (H/M = 0.7). H/M generally denotes hydrogen uptake from the fabricated materials. The H/M level is low, making them ideal for high-quality hydrogen storage materials due to their low affinity for hydrogen [92]. This increase in HE susceptibility with increased P concentration is typically caused by the intergranular segregation of P, which promotes H-induced intergranular cracking through additive or synergistic actions, or by P enhancing H absorption [89,93]. HEAs containing FENiCoCrMn was fabricated and experimented for HE susceptibility. The addition of Mn to the FeNiCoCr alloy system in cryogenic (−196 °C) temperature at different strain conditions (at cold rolled conditions like 15%, 30%, and 45% of strains) and their morphologies are shown in Fig. 14. In that figure, white dashed lines indicate grain boundaries (GBs), and a red circle indicates deformation twins (DTs). At 45%, more intense twinning forms and nano-twins develop into clusters and bundles to raise the strain rate from 15% to 45% [94].

For hydrogen accumulation, a single face-centered cubic (FCC) phase reduces the local micromechanical contrast. The solid solution's elements slow down the diffusion of hydrogen, preventing the production of hydride. With the help of alloying additions, the formation of nanotwins is better for making the work-hardening behaviour better when hydrogen is added. The low stacking fault energy aids in nanotwin formation. The dense surface oxide coating can increase the HE resistance by preventing hydrogen absorption [83]. During the deformation process, Mo can encourage the formation of c (NTs) in the hydrogen-charged specimen. When NTs engage with dislocation, they can prevent the local accumulation of hydrogen and disrupt the GBs' perpetual motion, which prevents intergranular decohesion and enhances the HE resistance. The formation of NTs in an alloy system subsequently reduces the development of failure in a sample, such as crack formation. Mn, Mo, and other elements are added to the alloy system to boost the hydrogen-enhanced local plasticity, aided by NTs. Elements like Ni and Fe metals, which have absorbed hydrogen, exhibit low hydrogen solubility at atmospheric pressure and temperature. These elements have a low critical hydrogen content and a low part per million in weight (wt. ppm). The range between wt. ppm <2 lower levels affect the ultimate tensile strength (UTS). The influence of hydrogen significantly impacts the UTS when the weight ppm exceeds 5 [95]. In automotive applications, the hydrogen concentration has wt. ppm <1 for a better optimum condition for the mitigation of HE [96]. When Ti is added to a multicomponent alloying system (HEAs), it makes the system easier to shape and absorbs hydrogen. This changes the phase from HCP (α-Ti) to BCC at high temperatures [56]. The HEAs based on $(FeCoNi)_{86}Al_7Ti_7$, with an average grain size of 42.3 mm was fabricated using vacuum arc melting process and was subjected to precipitation hardening under various aging conditions. Fig. 15(a) explains the effects of various thermodynamic processes under different heat treatment conditions. Fig. 15(b) indicates the Inverse Pole Figure (IPF) elements with random distribution natures. Fig. 15(c) indicates the Twin boundary formation with the help of annealing. Grain boundaries guide the identification of the twin locations. Reports indicate that the brittle L12 phase enhances the alloy's strength, subsequently reducing its ductility. Therefore, the imbalanced phase contributes to the transition from brittle to ductile. Fig. 15 (d) indicates the grain size distribution. Fig. 15 (e–f) presents the misorientation angle distribution and XRD results to confirm that alloys are FCC + L12 phases [74].

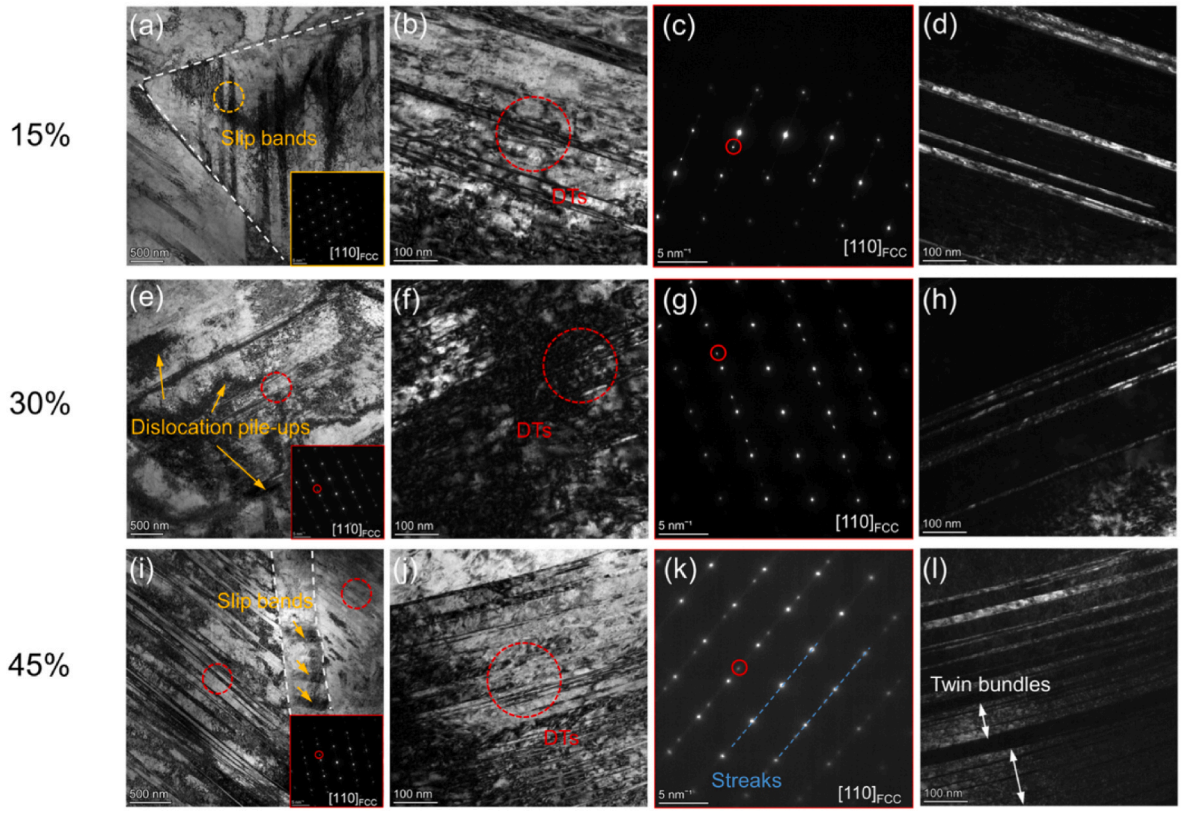

Fig. 14. Twinning morphologies in various strain rates (a–d) 15%, (e–h)30 %, (i–l) 45% of strains [94]. Reuse with journal permission. Copyrights 2024, Elsevier.

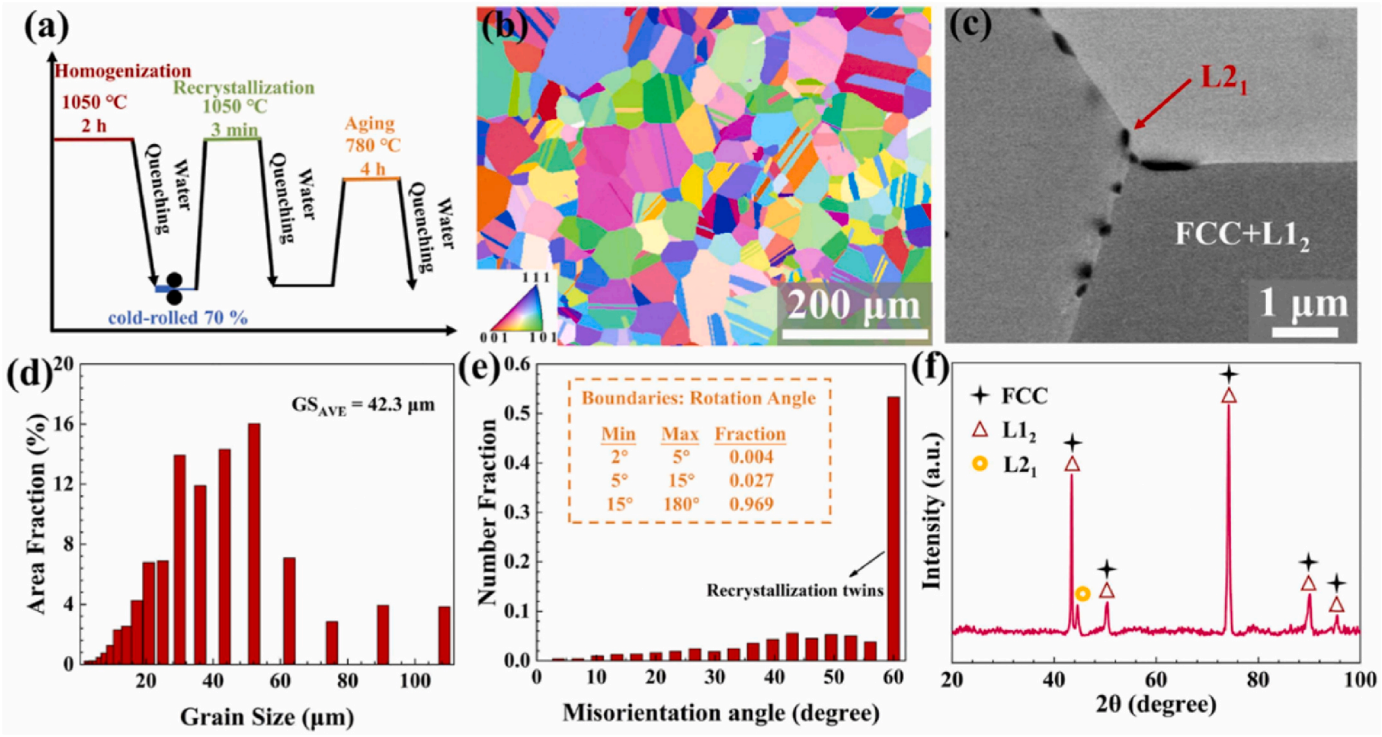

Fig. 15. (a) Heat treatment process of $(FeCoNi)_{86}Al_7Ti_7$ HEAs. (b) IPF based on EBST results. (c) FCC + $L1_2$ crystal structure. (d) Grain size distribution chart with the help of EBST results. (e) Recrystallization twins evaluation with the help of EBST misorientation angle distribution. (f) XRD results of HEAs [74]. Reuse with journal permission. Copyrights 2024, Elsevier.

9. Conclusion

This review identified recent developments in mitigating strategies for hydrogen embrittlement behaviour in hydrogen storage equipment using the high-entropy alloy concept. Adding multiple elements to increase the entropy level, which supports high-phase stability in all environmental conditions is an important reason for using HEAs to mitigate HE failures. The next-generation hydrogen storage systems focus on high hydrogen storage capacity, increased energy density capacity, high phase stability in moderate environmental conditions, and good cycling performance. In this direction, HEAs are most suitable for hydrogen storage tank development. The high hydrogen storage capacity and fast diffusion kinetics play major roles in the effective storage of hydrogen materials. In this direction, the selection of alloying elements decides the high storage capacity and diffusion kinetics. The addition of alloying elements like Co has a strong affinity to hydrogen, high reversibility, and high corrosion resistance, which is beneficial for using a high life span. The addition of Fe to HEAs promotes the hydride formation to achieve a high volumetric energy density and maintain a low-pressure level inside the hydrogen storage equipment. But more % of Fe addition to other alloys has a higher chance of developing a failure and loss of mechanical strength. To overcome this aspect, Ni is added to resist the HE failure because Ni is a good austenitic stabilizer, and either with or without hydrogen conditions the stable grain structure is maintained. The inclusion of Mn in HEAs aims to develop a nanosized twin formation inside the alloy system. The twins eliminate the dislocation motion, which also improves the strengthening behaviour of the alloy system. The multi-component alloys eliminate the crystal structure changes (to BCC) followed by intergranular cracks developing inside the grain boundaries and ensure high-phase stability in a hydrogen-induced environment.

Declaration of competing interest

The authors declare that they have no known competing financial interests or personal relationships that could have appeared to influence the work reported in this paper.

Nomenclature section:

AIDE	Adsorption Induced Dislocation Emission
AM	Arc Melting
APT	Atom probe tomography
ASTM	American society for testing and Materials
BCC	Body centered cubic
BM	Ball Milling
CG	Coarse grain
COP	Complex ordered phase
DHF	Decohesive hydrogen fracture
DLMD	Direct laser Metal deposition
DTs	Deformation twins
EE	Environmental embrittlement

(*continued on next page*)

(*continued*)

EHE	External hydrogen embrittlement
EI	Embrittlement index
FCC	Face centered cubic
FG	Fine grain
HAC	Hydrogen assisted cracking
HAM	Hydrogen changed Micro fracture Mode
HCP	Hexagonal close Packed
HDMC	Hydrogen assisted Micro void coalescence
HE	Hydrogen embrittlement
HEV	Hydrogen evaporation
HEAs	High entropy alloys
HEBM	High energy ball Milling
HEDE	Hydrogen enhanced de cohesion Mechanism
HELP	Hydrogen enhanced local plasticity Model
HEMD	Hydrogen enhanced Macroscopic ductility
HIC	Hydrogen induced cracking
HMT	Hydrogen Micro print techniques
HT	Hydrogen trapping
HTHA	High temperature hydrogen attack
IHE	Internal hydrogen implantation
IPCC	Intergovernmental panel on Climate change
IPF	Inverse Pole Figure
ITE	Intermediate temperature embrittlement
LDE	Lattice distortion effects
LENS	Laser engineered net shaping
MF	Mixed fracture
MS	Melt spinning
MVC	Micro void coalescence
Dts	Deformation twins
SDP	Simple disordered phase
SEM	Scanning electron Microscopy
SFE	Stacking fault energy
SIMS	Secondary iron Mass spectroscopy
SLD	Sluggish diffusion
SOP	Simple ordered phase
SS	Simple solid solution
TDS	Thermal desorption spectroscopy
UTS	Ultimate tensile strength
VEC	Valence electron concentration
WHR	Work hardening rate
XRD	X Ray Diffraction

References

[1] Yang D, et al. A novel FeCrNiAlTi-based high entropy alloy strengthened by refined grains. J Alloys Compd May 2020;823:153729. https://doi.org/10.1016/j.jallcom.2020.153729.

[2] Balaji V, Xavior AM. Effects of high entropy alloys coating (HEAC) and their property evaluation. J Appl Sci Eng 2024;27(11):3485–98. https://doi.org/10.6180/jase.202411_27(11).0012.

[3] Gupta M. An insight into the development of light weight high entropy alloys. Res. Dev. Mater. Sci. Nov. 2017;2(2). https://doi.org/10.31031/RDMS.2017.02.000534.

[4] Kumar A, Singh A, Suhane A. Mechanically alloyed high entropy alloys: existing challenges and opportunities. J Mater Res Technol Mar. 2022;17:2431–56. https://doi.org/10.1016/j.jmrt.2022.01.141.

[5] Lv Y, et al. A novel high entropy alloy with outstanding strength by low temperature annealing after severe cold rolling. J Mater Res Technol Jan. 2024;28:4358–62. https://doi.org/10.1016/j.jmrt.2024.01.004.

[6] Huang A, Fensin SJ, Meyers MA. Strain-rate effects and dynamic behavior of high entropy alloys. J Mater Res Technol Jan. 2023;22:307–47. https://doi.org/10.1016/j.jmrt.2022.11.057.

[7] Xin Y, et al. High-entropy alloys as a platform for catalysis: progress, challenges, and opportunities. ACS Catal Oct. 2020;10(19):11280–306. https://doi.org/10.1021/acscatal.0c03617.

[8] V B, X M A. Development of high entropy alloys (HEAs): current trends. Heliyon 2024:e26464. https://doi.org/10.1016/j.heliyon.2024.e26464. November 2023.

[9] Somo TR, Lototskyy MV, Yartys VA, Davids MW, Nyamsi SN. Hydrogen storage behaviours of high entropy alloys: a Review. J Energy Storage Dec. 2023;73:108969. https://doi.org/10.1016/j.est.2023.108969.

[10] Luo L, et al. High-entropy alloys for solid hydrogen storage: a review. Int J Hydrogen Energy Jan. 2024;50:406–30. https://doi.org/10.1016/j.ijhydene.2023.07.146.

[11] Brandon NP, Kurban Z. Clean energy and the hydrogen economy. Philos. Trans. R. Soc. A Math. Phys. Eng. Sci. Jul. 2017;375(2098):20160400. https://doi.org/10.1098/rsta.2016.0400.

[12] Sahlberg M, Karlsson D, Zlotea C, Jansson U. Superior hydrogen storage in high entropy alloys. Sci Rep Nov. 2016;6(1):36770. https://doi.org/10.1038/srep36770.

[13] Xin X, Johansson R, Wolff M, Hjörvarsson B. Hydrogen in vanadium: site occupancy and isotope effects. Phys Rev B Apr. 2016;93(13):134107. https://doi.org/10.1103/PhysRevB.93.134107.

[14] Ren C, Sun K, Jia YF, Zhang NZ, Jia YD, Wang G. Effect of Mo addition on the microstructural evolution and mechanical properties of Fe–Ni–Cr–Mn–Al–Ti high entropy alloys. Mater. Sci. Eng. A Feb. 2023;864:144579. https://doi.org/10.1016/j.msea.2023.144579.

[15] Niaz S, Manzoor T, Pandith AH. Hydrogen storage: materials, methods and perspectives. Renew Sustain Energy Rev Oct. 2015;50:457–69. https://doi.org/10.1016/j.rser.2015.05.011.

[16] Moradi R, Groth KM. Hydrogen storage and delivery: review of the state of the art technologies and risk and reliability analysis. Int J Hydrogen Energy May 2019;44(23):12254–69. https://doi.org/10.1016/j.ijhydene.2019.03.041.

[17] Storage of pure hydrogen in different states. In: Hydrogen storage technologies. Wiley; 2012. p. 97–170. https://doi.org/10.1002/9783527649921.ch4.

[18] Meda US, Bhat N, Pandey A, Subramanya KN, Lourdu Antony Raj MA. Challenges associated with hydrogen storage systems due to the hydrogen embrittlement of high strength steels. Int J Hydrogen Energy Jun. 2023;48(47):17894–913. https://doi.org/10.1016/j.ijhydene.2023.01.292.

[19] Dillon AC, Heben MJ. Hydrogen storage using carbon adsorbents: past, present and future. Appl Phys Mater Sci Process Feb. 2001;72(2):133–42. https://doi.org/10.1007/s003390100788.

[20] Satyapal S, Petrovic J, Read C, Thomas G, Ordaz G. The U.S. Department of energy's national hydrogen storage project: progress towards meeting hydrogen-powered vehicle requirements. Catal Today Feb. 2007;120(3–4):246–56. https://doi.org/10.1016/j.cattod.2006.09.022.

[21] Wang S, Xu DK, Zhang ZQ, Ma YJ, Qiao YX. Effect of electrochemical hydrogen charging on the mechanical behavior of a dual-phase Ti–4Al–2V–1Mo–1Fe (in wt. %) alloy. Mater. Sci. Eng. A Jan. 2021;802:140448. https://doi.org/10.1016/j.msea.2020.140448.

[22] Koren E, Hagen CMH, Wang D, Lu X, Johnsen R, Yamabe J. Experimental comparison of gaseous and electrochemical hydrogen charging in X65 pipeline

steel using the permeation technique. Corros. Sci. May 2023;215:111025. https://doi.org/10.1016/j.corsci.2023.111025.
[23] Röthig M, Hoschke J, Tapia C, Venezuela J, Atrens A. A review of gas phase inhibition of gaseous hydrogen embrittlement in pipeline steels. Int J Hydrogen Energy Mar. 2024;60:1239–65. https://doi.org/10.1016/j.ijhydene.2024.02.245.
[24] Pu Z, Chen Y, Dai LH. Strong resistance to hydrogen embrittlement of high-entropy alloy. Mater. Sci. Eng. A Oct. 2018;736:156–66. https://doi.org/10.1016/j.msea.2018.08.101.
[25] Kim Y-K, Suh J-Y, Lee K-A. Effect of gaseous hydrogen embrittlement on the mechanical properties of additively manufactured CrMnFeCoNi high-entropy alloy strengthened by in-situ formed oxide. Mater. Sci. Eng. A Oct. 2020;796:140039. https://doi.org/10.1016/j.msea.2020.140039.
[26] Dąbrowa J, et al. Demystifying the sluggish diffusion effect in high entropy alloys. J Alloys Compd Apr. 2019;783:193–207. https://doi.org/10.1016/j.jallcom.2018.12.300.
[27] Osman H, Liu L. Additive manufacturing of high-entropy alloy composites: a review. Trans. Nonferrous Met. Soc. China Jan. 2023;33(1):1–24. https://doi.org/10.1016/S1003-6326(22)66086-2.
[28] Gao MC, Yeh J-W, Liaw PK, Zhang Y, editors. High-entropy alloys. Cham: Springer International Publishing; 2016. https://doi.org/10.1007/978-3-319-27013-5.
[29] Yin KX, Dong GY, Zhang GJ, Tian QW, Wang YN, Huang JC. Prediction of phase structures of solid solutions for high entropy alloys. J Mater Res Technol May 2023;24:7654–65. https://doi.org/10.1016/j.jmrt.2023.04.191.
[30] Miracle DB, Senkov ON. A critical review of high entropy alloys and related concepts. Acta Mater Jan. 2017;122:448–511. https://doi.org/10.1016/j.actamat.2016.08.081.
[31] Koyama T, Tsukada Y, Abe T. Simple approach for evaluating the possibility of sluggish diffusion in high-entropy alloys. J Phase Equilibria Diffus Feb. 2022;43(1):68–77. https://doi.org/10.1007/s11669-022-00938-9.
[32] Ferraz M de B, Botta WJ, Zepon G. Synthesis, characterization and first hydrogen absorption/desorption of the Mg35Al15Ti25V10Zn15 high entropy alloy. Int J Hydrogen Energy Jun. 2022;47(54):22881–92. https://doi.org/10.1016/j.ijhydene.2022.05.098.
[33] Montero J, et al. Hydrogen storage properties of the refractory Ti–V–Zr–Nb–Ta multi-principal element alloy. J Alloys Compd Sep. 2020;835:155376. https://doi.org/10.1016/j.jallcom.2020.155376.
[34] Montero J, Ek G, Laversenne L, Nassif V, Sahlberg M, Zlotea C. How 10 at% Al addition in the Ti-V-Zr-Nb high-entropy alloy changes hydrogen sorption properties. Molecules Apr. 2021;26(9):2470. https://doi.org/10.3390/molecules26092470.
[35] Dewangan SK, Sharma VK, Sahu P, Kumar V. Synthesis and characterization of hydrogenated novel AlCrFeMnNiW high entropy alloy. Int J Hydrogen Energy Jul. 2020;45(34):16984–91. https://doi.org/10.1016/j.ijhydene.2019.08.113.
[36] Zepon G, et al. Hydrogen-induced phase transition of MgZrTiFe0.5Co0.5Ni0.5 high entropy alloy. Int J Hydrogen Energy Jan. 2018;43(3):1702–8. https://doi.org/10.1016/j.ijhydene.2017.11.106.
[37] Marques F, et al. Mg-containing multi-principal element alloys for hydrogen storage: a study of the MgTiNbCr0.5Mn0.5Ni0.5 and Mg0.68TiNbNi0.55 compositions. Int J Hydrogen Energy Jul. 2020;45(38):19539–52. https://doi.org/10.1016/j.ijhydene.2020.05.069.
[38] Karlsson D, et al. Structure and hydrogenation properties of a HfNbTiVZr high-entropy alloy. Inorg Chem Feb. 2018;57(4):2103–10. https://doi.org/10.1021/acs.inorgchem.7b03004.
[39] Nygård MM, Ek G, Karlsson D, Sahlberg M, Sørby MH, Hauback BC. Hydrogen storage in high-entropy alloys with varying degree of local lattice strain. Int J Hydrogen Energy Nov. 2019;44(55):29140–9. https://doi.org/10.1016/j.ijhydene.2019.03.223.
[40] Ek G, et al. Elucidating the effects of the composition on hydrogen sorption in TiVZrNbHf-based high-entropy alloys. Inorg Chem Jan. 2021;60(2):1124–32. https://doi.org/10.1021/acs.inorgchem.0c03270.
[41] Shen H, et al. A novel TiZrHfMoNb high-entropy alloy for solar thermal energy storage. Nanomaterials Feb. 2019;9(2):248. https://doi.org/10.3390/nano9020248.
[42] Zadorozhnyy V, et al. Composition design, synthesis and hydrogen storage ability of multi-principal-component alloy TiVZrNbTa. J Alloys Compd Apr. 2022;901:163638. https://doi.org/10.1016/j.jallcom.2022.163638.
[43] Kao Y-F, et al. Hydrogen storage properties of multi-principal-component CoFeMnTixVyZrz alloys. Int J Hydrogen Energy Sep. 2010;35(17):9046–59. https://doi.org/10.1016/j.ijhydene.2010.06.012.
[44] Chen S-K, Lee P-H, Lee H, Su H-T. Hydrogen storage of C14-CruFevMnwTixVyZrz alloys. Mater Chem Phys May 2018;210:336–47. https://doi.org/10.1016/j.matchemphys.2017.08.008.
[45] Chen J, et al. Superior cycle life of TiZrFeMnCrV high entropy alloy for hydrogen storage. Scr. Mater. Apr. 2022;212:114548. https://doi.org/10.1016/j.scriptamat.2022.114548.
[46] Tsai K-Y, Tsai M-H, Yeh J-W. Sluggish diffusion in Co–Cr–Fe–Mn–Ni high-entropy alloys. Acta Mater Aug. 2013;61(13):4887–97. https://doi.org/10.1016/j.actamat.2013.04.058.
[47] Mehta A, Sohn YH. Fundamental core effects in transition metal high-entropy alloys: 'high-entropy' and 'sluggish diffusion' effects. Diffus Found Apr. 2021;29:75–93. 10.4028/www.scientific.net/DF.29.75.
[48] Mehta A, Sohn Y. High entropy and sluggish diffusion 'core' effects in senary FCC Al–Co–Cr–Fe–Ni–Mn alloys. ACS Comb Sci Dec. 2020;22(12):757–67. https://doi.org/10.1021/acscombsci.0c00096.
[49] Wang L, et al. Surprising cocktail effect in high entropy alloys on catalyzing magnesium hydride for solid-state hydrogen storage. Chem. Eng. J. Jun. 2023;465:142766. https://doi.org/10.1016/j.cej.2023.142766.
[50] Zhang F, Zhang C, Chen SL, Zhu J, Cao WS, Kattner UR. An understanding of high entropy alloys from phase diagram calculations. Calphad Jun. 2014;45:1–10. https://doi.org/10.1016/j.calphad.2013.10.006.
[51] Luo H, Li Z, Raabe D. Hydrogen enhances strength and ductility of an equiatomic high-entropy alloy. Sci Rep Aug. 2017;7(1):9892. https://doi.org/10.1038/s41598-017-10774-4.
[52] Li X, et al. Design of (Nb, Mo)40Ti30Ni30 alloy membranes for combined enhancement of hydrogen permeability and embrittlement resistance. Sci Rep Mar. 2017;7(1):209. https://doi.org/10.1038/s41598-017-00335-0.
[53] Lynch SP. Metallographic and fractographic techniques for characterising and understanding hydrogen-assisted cracking of metals. In: Gaseous hydrogen embrittlement of materials in energy technologies. Elsevier; 2012. p. 274–346. https://doi.org/10.1533/9780857093899.2.274.
[54] Song J, Curtin WA. Atomic mechanism and prediction of hydrogen embrittlement in iron. Nat Mater Feb. 2013;12(2):145–51. https://doi.org/10.1038/nmat3479.
[55] Dwivedi SK, Vishwakarma M. Hydrogen embrittlement in different materials: a review. Int J Hydrogen Energy Nov. 2018;43(46):21603–16. https://doi.org/10.1016/j.ijhydene.2018.09.201.
[56] Chen Y-S, et al. Hydrogen trapping and embrittlement in metals – a review. Int J Hydrogen Energy Apr. 2024. https://doi.org/10.1016/j.ijhydene.2024.04.076.
[57] Kirchheim R. Reducing grain boundary, dislocation line and vacancy formation energies by solute segregationII. Experimental evidence and consequences. Acta Mater Sep. 2007;55(15):5139–48. https://doi.org/10.1016/j.actamat.2007.05.033.
[58] Kappes M, Iannuzzi M, Carranza RM. Hydrogen embrittlement of magnesium and magnesium alloys: a review. J Electrochem Soc Feb. 2013;160(4):C168–78. https://doi.org/10.1149/2.023304jes.
[59] Lynch SP. Hydrogen embrittlement (HE) phenomena and mechanisms. In: Stress corrosion cracking. Elsevier; 2011. p. 90–130. https://doi.org/10.1533/9780857093769.1.90.
[60] Robertson IM. The effect of hydrogen on dislocation dynamics. Eng Fract Mech Nov. 1999;64(5):649–73. https://doi.org/10.1016/S0013-7944(99)00094-6.
[61] Pundt A, Kirchheim R. Hydrogen in metals: microstructural aspects. Annu Rev Mater Res Aug. 2006;36(1):555–608. https://doi.org/10.1146/annurev.matsci.36.090804.094451.
[62] Venezuela J, et al. The influence of microstructure on the hydrogen embrittlement susceptibility of martensitic advanced high strength steels. Mater Today Commun Dec. 2018;17:1–14. https://doi.org/10.1016/j.mtcomm.2018.07.011.
[63] Silverstein R, Eliezer D, Tal-Gutelmacher E. Hydrogen trapping in alloys studied by thermal desorption spectrometry. J Alloys Compd May 2018;747:511–22. https://doi.org/10.1016/j.jallcom.2018.03.066.
[64] Venezuela J, Zhou Q, Liu Q, Zhang M, Atrens A. Hydrogen trapping in some automotive martensitic advanced high-strength steels. Adv Eng Mater Jan. 2018;20(1). https://doi.org/10.1002/adem.201700468.
[65] Atrens A, Liu Q, Zhou Q, Venezuela J, Zhang M. Evaluation of automobile service performance using laboratory testing. Mater Sci Technol Oct. 2018;34(15):1893–909. https://doi.org/10.1080/02670836.2018.1495903.
[66] Atrens A, et al. Influence of hydrogen on steel components for clean energy. Corros. Mater. Degrad. Jun. 2018;1(1):3–26. https://doi.org/10.3390/cmd1010002.
[67] de Guzman Venezuela JJ. The influence of hydrogen on MS980, MS1180, MS1300 and MS1500 martensitic advanced high strength steels used for automotive applications. The University of Queensland; 2017. https://doi.org/10.14264/uql.2017.799.
[68] Chen Y-S, et al. Atom probe tomography for the observation of hydrogen in materials: a review. Microsc Microanal Feb. 2023;29(1):1–15. https://doi.org/10.1093/micmic/ozac005.
[69] Shen Y, Howard L, Yu X-Y. Secondary ion mass spectral imaging of metals and alloys. Materials Jan. 2024;17(2):528. https://doi.org/10.3390/ma17020528.
[70] Guan K, Szpunar JA, Matocha K, Wang D. Study on temper embrittlement and hydrogen embrittlement of a hydrogenation reactor by small punch test. Materials Jun. 2017;10(6):671. https://doi.org/10.3390/ma10060671.
[71] Chen Y, Zhao S, Ma H, Wang H, Hua L, Fu S. Analysis of hydrogen embrittlement on aluminum alloys for vehicle-mounted hydrogen storage tanks: a review. Metals Aug. 2021;11(8):1303. https://doi.org/10.3390/met11081303.
[72] Hoschke J, Chowdhury MFW, Venezuela J, Atrens A. A review of hydrogen embrittlement in gas transmission pipeline steels. Corros. Rev. Jun. 2023;41(3):277–317. https://doi.org/10.1515/corrrev-2022-0052.
[73] Zhao Y, et al. Resistance of CoCrFeMnNi high-entropy alloy to gaseous hydrogen embrittlement. Scr. Mater. Jul. 2017;135:54–8. https://doi.org/10.1016/j.scriptamat.2017.03.029.
[74] Cheng H, Luo H, Pan Z, Wang X, Zhao Q, Li X. Hydrogen embrittlement of a precipitation-strengthened high-entropy alloy. Corros. Sci. Feb. 2024;227:111708. https://doi.org/10.1016/j.corsci.2023.111708.
[75] Koyama M, Ichii K, Tsuzaki K. Grain refinement effect on hydrogen embrittlement resistance of an equiatomic CoCrFeMnNi high-entropy alloy. Int J Hydrogen Energy Jun. 2019;44(31):17163–7. https://doi.org/10.1016/j.ijhydene.2019.04.280.
[76] Kissinger HE. Reaction kinetics in differential thermal analysis. Anal Chem Nov. 1957;29(11):1702–6. https://doi.org/10.1021/ac60131a045.
[77] Li X, Ma X, Zhang J, Akiyama E, Wang Y, Song X. Review of hydrogen sm and PreventionEmbrittlement in metals: hydrogen diffusion, hydrogen characterization, hydrogen embrittlement mechani. Acta Metall. Sin. (English Lett. Jun. 2020;33(6):759–73. https://doi.org/10.1007/s40195-020-01039-7.

[78] Zhou C, Ye B, Song Y, Cui T, Xu P, Zhang L. Effects of internal hydrogen and surface-absorbed hydrogen on the hydrogen embrittlement of X80 pipeline steel. Int J Hydrogen Energy Aug. 2019;44(40):22547–58. https://doi.org/10.1016/j.ijhydene.2019.04.239.
[79] Li X, Dao M, Eberl C, Hodge AM, Gao H. Fracture, fatigue, and creep of nanotwinned metals. MRS Bull 2016;41(4):298–304. https://doi.org/10.1557/mrs.2016.65.
[80] Pradhan A, Vishwakarma M, Dwivedi SK. A review: the impact of hydrogen embrittlement on the fatigue strength of high strength steel. Mater Today Proc 2020;26:3015–9. https://doi.org/10.1016/j.matpr.2020.02.627.
[81] Lee J, Park H, Kim M, Kim H-J, Suh J, Kang N. Role of hydrogen and temperature in hydrogen embrittlement of equimolar CoCrFeMnNi high-entropy alloy. Met Mater Int Jan. 2021;27(1):166–74. https://doi.org/10.1007/s12540-020-00752-3.
[82] Khare A, Vishwakarma M, Parashar V. A review on failures of industrial components due to hydrogen embrittlement & techniques for damage prevention. Int J Appl Eng Res 2017;12(8):1784–92.
[83] Luo H, et al. A strong and ductile medium-entropy alloy resists hydrogen embrittlement and corrosion. Nat Commun Jun. 2020;11(1):3081. https://doi.org/10.1038/s41467-020-16791-8.
[84] Park I-J, Jo SY, Kang M, Lee S-M, Lee Y-K. The effect of Ti precipitates on hydrogen embrittlement of Fe–18Mn–0.6C–2Al–xTi twinning-induced plasticity steel. Corros. Sci. Dec. 2014;89:38–45. https://doi.org/10.1016/j.corsci.2014.08.005.
[85] Alam I, Adaan-Nyiak MA, Tiamiyu AA. Revisiting the phase stability rules in the design of high-entropy alloys: a case study of quaternary alloys produced by mechanical alloying. Intermetallics Aug. 2023;159:107919. https://doi.org/10.1016/j.intermet.2023.107919.
[86] Otto F, Yang Y, Bei H, George EP. Relative effects of enthalpy and entropy on the phase stability of equiatomic high-entropy alloys. Acta Mater Apr. 2013;61(7):2628–38. https://doi.org/10.1016/j.actamat.2013.01.042.
[87] Cho S, et al. Comparison of hydrogen embrittlement susceptibility of different types of advanced high-strength steels. Materials May 2022;15(9):3406. https://doi.org/10.3390/ma15093406.
[88] Wang J, Liu X, Hu J, Tian Y, Xi X, Chen L. Optimizing the hydrogen embrittlement resistance by Cu addition in a low carbon high strength steel. Eng Fail Anal Apr. 2024;158:108004. https://doi.org/10.1016/j.engfailanal.2024.108004.
[89] Dieudonné T, et al. Role of copper and aluminum additions on the hydrogen embrittlement susceptibility of austenitic Fe–Mn–C TWIP steels. Corros. Sci. May 2014;82:218–26. https://doi.org/10.1016/j.corsci.2014.01.022.
[90] Sharma B, Harini S. A possibility of Pd based high entropy alloy for hydrogen gas sensing applications. Mater Res Express Nov. 2019;6(11):1165d7. https://doi.org/10.1088/2053-1591/ab4fae.
[91] Lu L, Ni J, Peng Z, Zhang H, Liu J. Hydrogen embrittlement and improved resistance of Al addition in twinning-induced plasticity steel: first-principles study. Materials Apr. 2019;12(8):1341. https://doi.org/10.3390/ma12081341.
[92] Strozi RB, Leiva DR, Huot J, Botta WJ, Zepon G. An approach to design single BCC Mg-containing high entropy alloys for hydrogen storage applications. Int J Hydrogen Energy Jul. 2021;46(50):25555–61. https://doi.org/10.1016/j.ijhydene.2021.05.087.
[93] Zhang C, Yu H, Zhi H, Antonov S, Su Y. Twinning behavior and hydrogen embrittlement of a pre-strained twinning-induced plasticity (TWIP) steel. Corros. Sci. Nov. 2021;192:109791. https://doi.org/10.1016/j.corsci.2021.109791.
[94] Guo Z, Yan Y. The role of cryogenic pre-strain on the hydrogen embrittlement of FeNiCoCrMn high-entropy alloys. Corros. Sci. 2023;218(April):111197. https://doi.org/10.1016/j.corsci.2023.111197.
[95] Lovicu G, et al. Hydrogen embrittlement of automotive advanced high-strength steels. Metall Mater Trans A Nov. 2012;43(11):4075–87. https://doi.org/10.1007/s11661-012-1280-8.
[96] Ootsuka S, Fujita S, Tada E, Nishikata A, Tsuru T. Evaluation of hydrogen absorption into steel in automobile moving environments. Corros. Sci. Sep. 2015;98:430–7. https://doi.org/10.1016/j.corsci.2015.05.049.

Dr. M. Anthony Xavior is a Professor in Manufacturing Department, School of Mechanical Engineering at Vellore Institute of Technology, Vellore, India. He has around 24 years of teaching and research experience at VIT, Vellore. His research specialization includes machinability study, development and property evaluation of metal matrix composites and metal additive manufacturing, development of novel materials for hydrogen storage and hydrogen embrittlement studies. He had received research grants from Department of Space, Aeronautics Research and Development Board (AR&DB) and Science and Engineering Research Board (SERB) Government of India respectively for the development of composites suitable for various applications. He has published around 200 papers in international and national journals and conference proceedings in the area of materials and manufacturing. He has produced eleven Doctorates and one Masters by Research in the field of metal matrix composites and machinability studies. He is a member of American Society of Mechanical Engineers (ASME), Life Member for Indian Society for Technical Education and Life Member of Institution of Engineers (India). He appears consistently in the list of Top 2% of Scientists in the world as per the study undertaken by Stanford University & Elsevier